

Parton Showers, Matching & Merging

Bryan Webber



UNIVERSITY OF
CAMBRIDGE

Outline

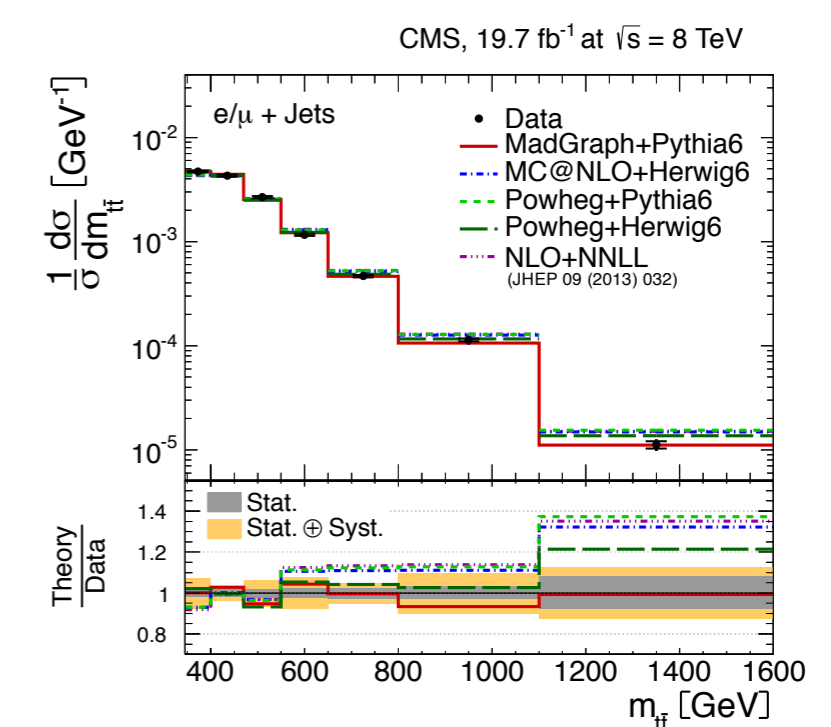
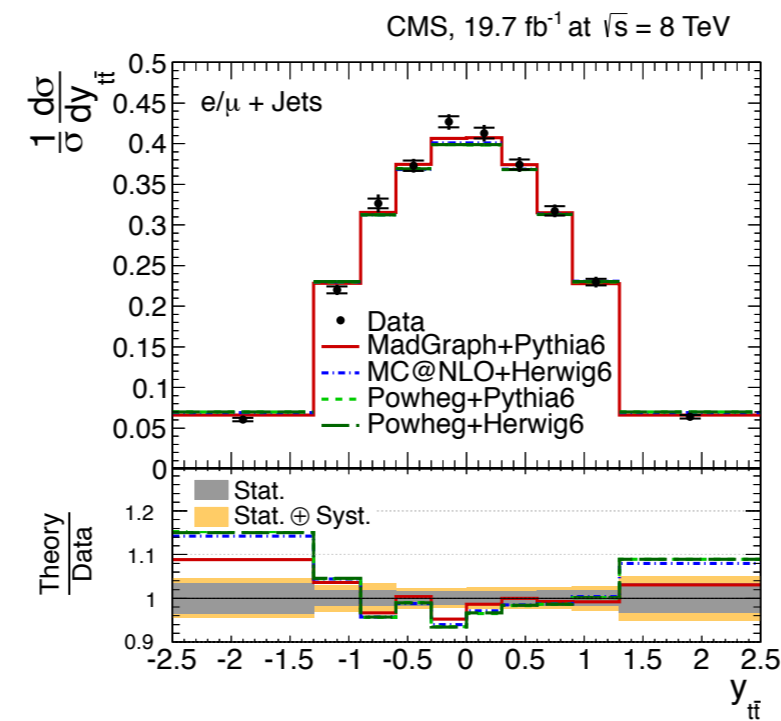
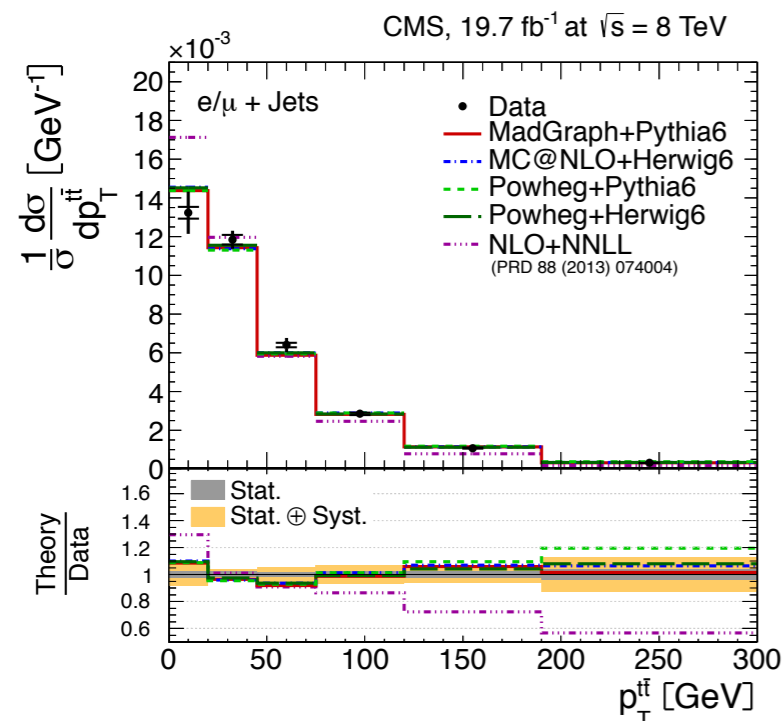
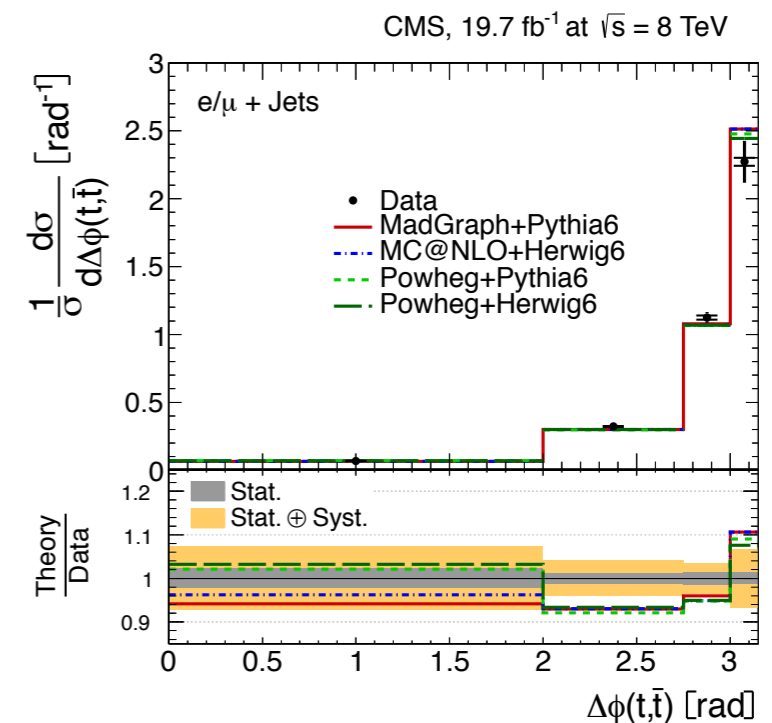
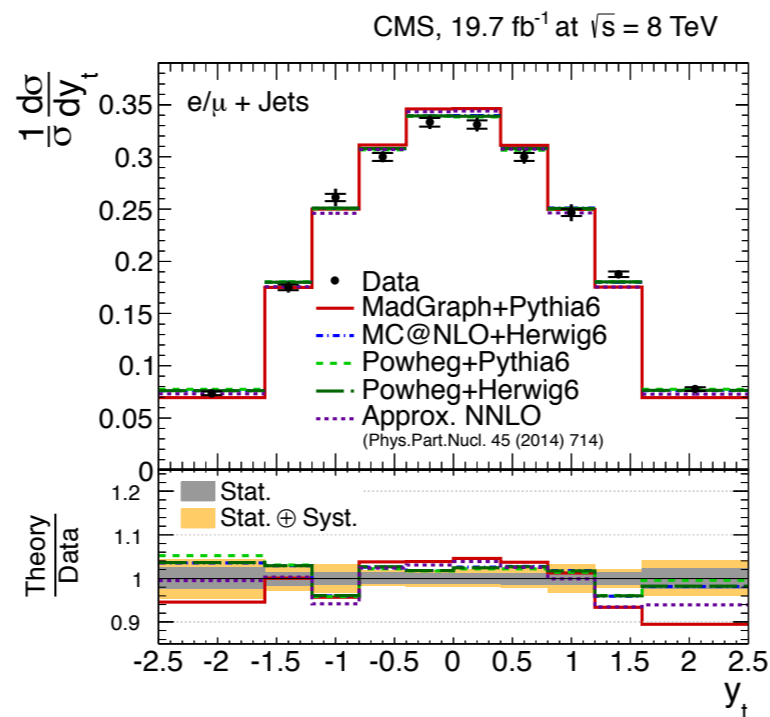
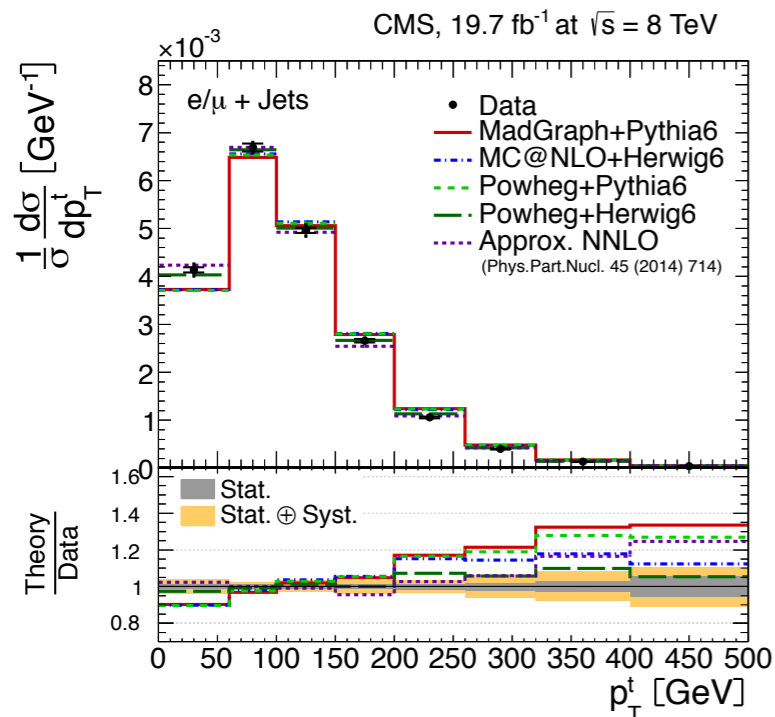
- Matching to a fixed order
 - ✦ NLO: MC@NLO, POWHEG, KrkNLO; automation
 - ✦ NNLO: NNLOPS, UN²LOPS, Geneva
- Matching to multiple fixed orders
 - ✦ MEPS@NLO, FxFx, UNLOPS, ...
- Shower variables and improvements
 - ✦ Coherence, colour, spin, ...
- Conclusions

NLO matching

NLO matching

- Full inclusive NLO, extra jet LO
- Still mostly MC@NLO or POWHEG
- MC@NLO:
 - ✦ PS-specific; beyond NLO is PS only; some negative weights
- POWHEG:
 - ✦ Any PS; extra terms beyond NLO; positive weights
- New: KrkNLO

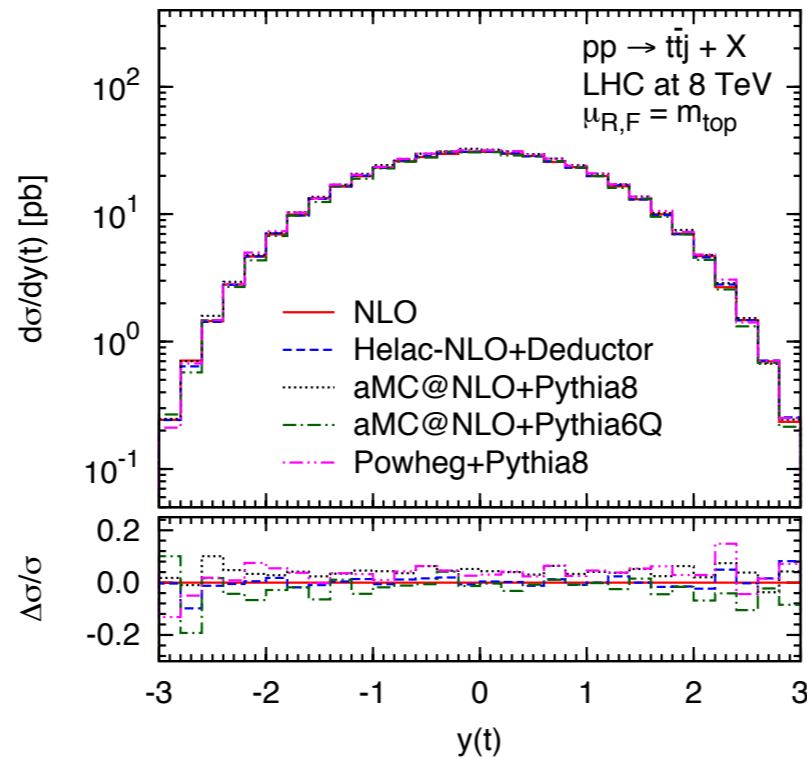
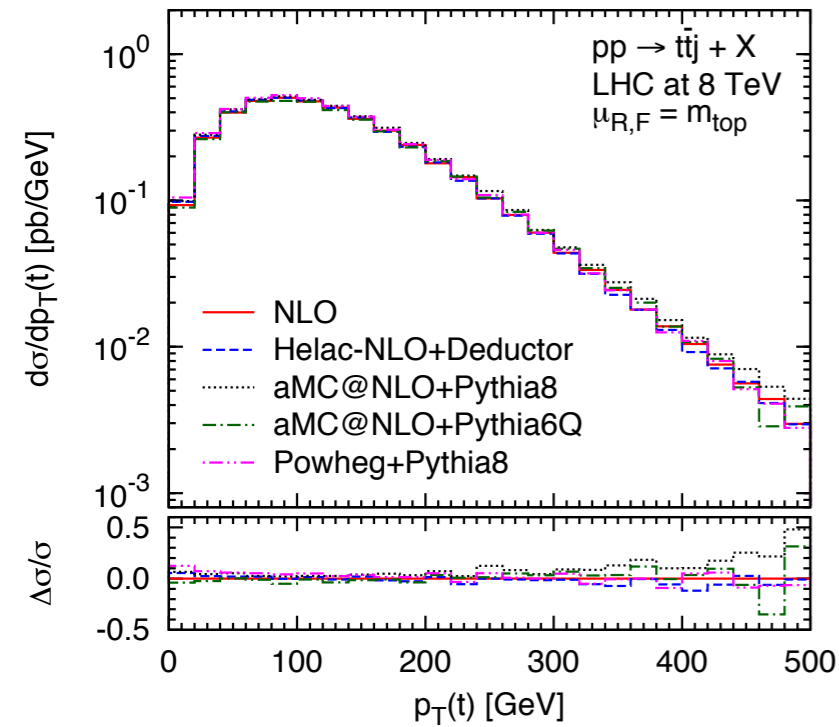
Top pairs at 8 TeV



● Differences are small!

CMS, I505.04480

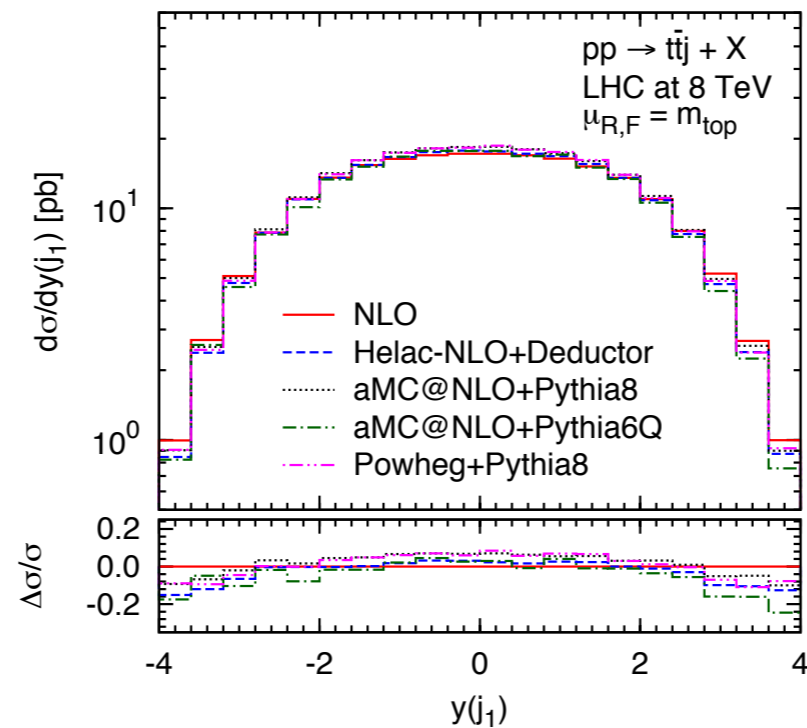
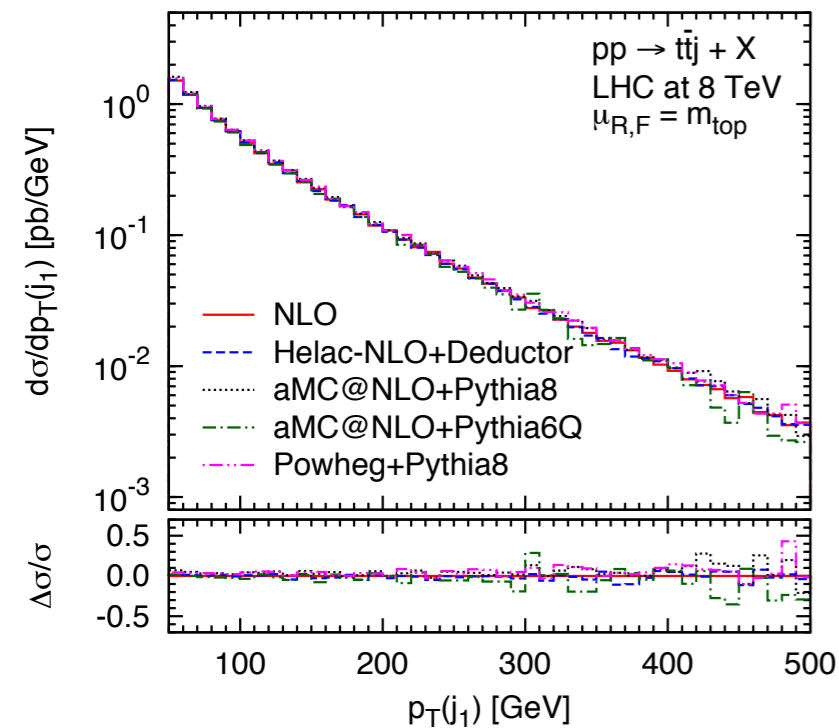
DEDUCTOR MC@NLO



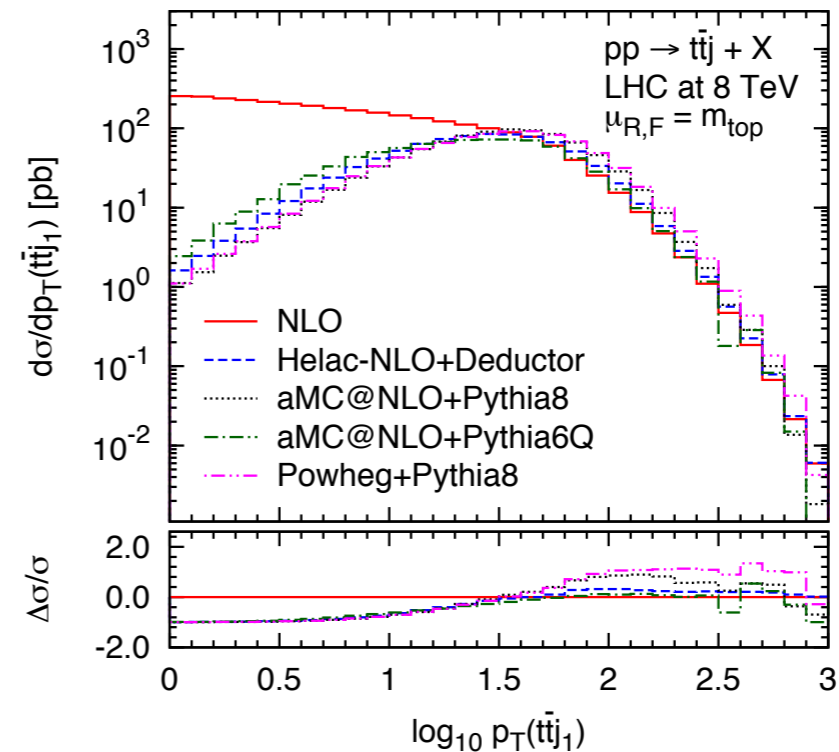
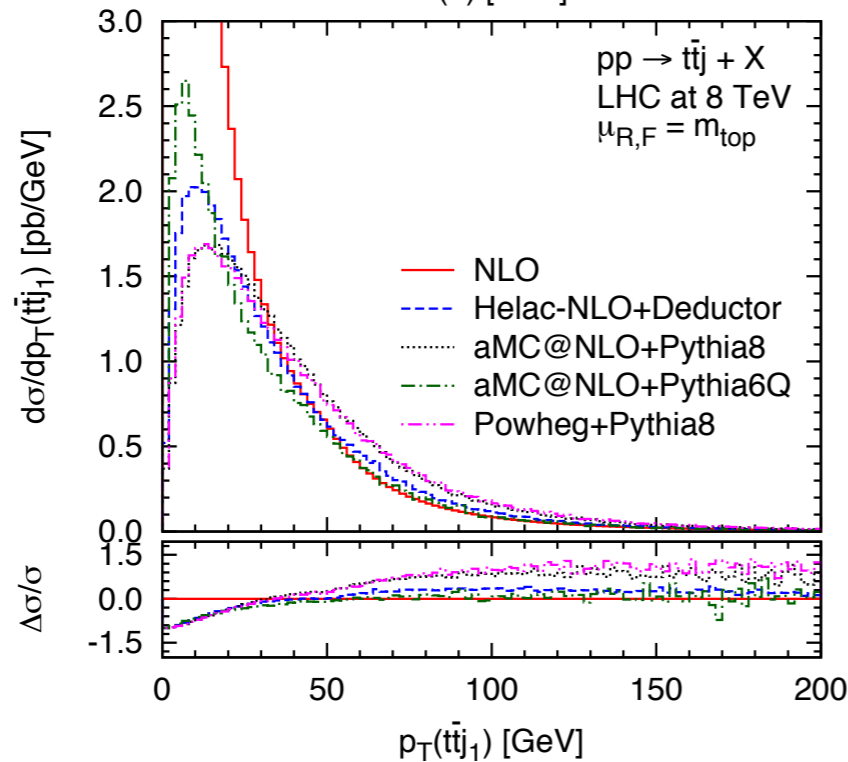
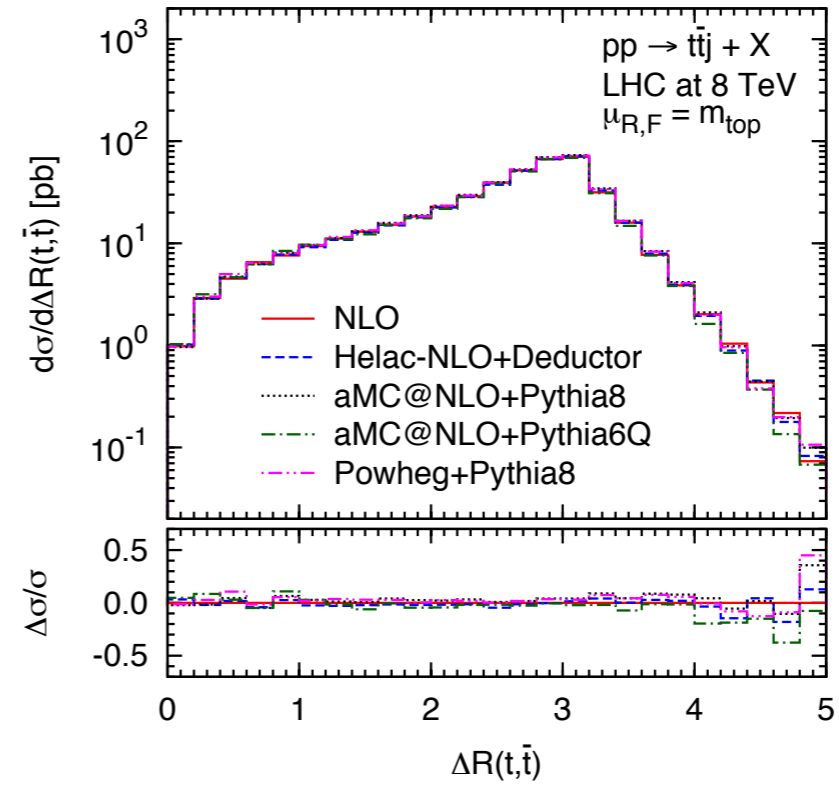
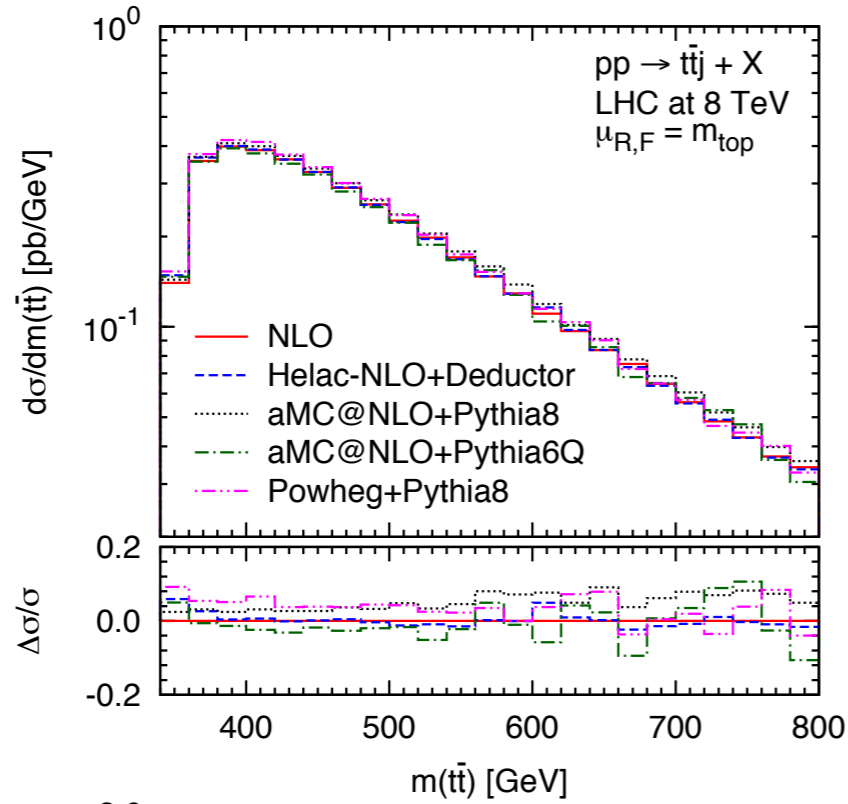
● $pp \rightarrow t\bar{t}j + X$

Nagy, Soper, I40I.6364

Czakon et al., I502.00925

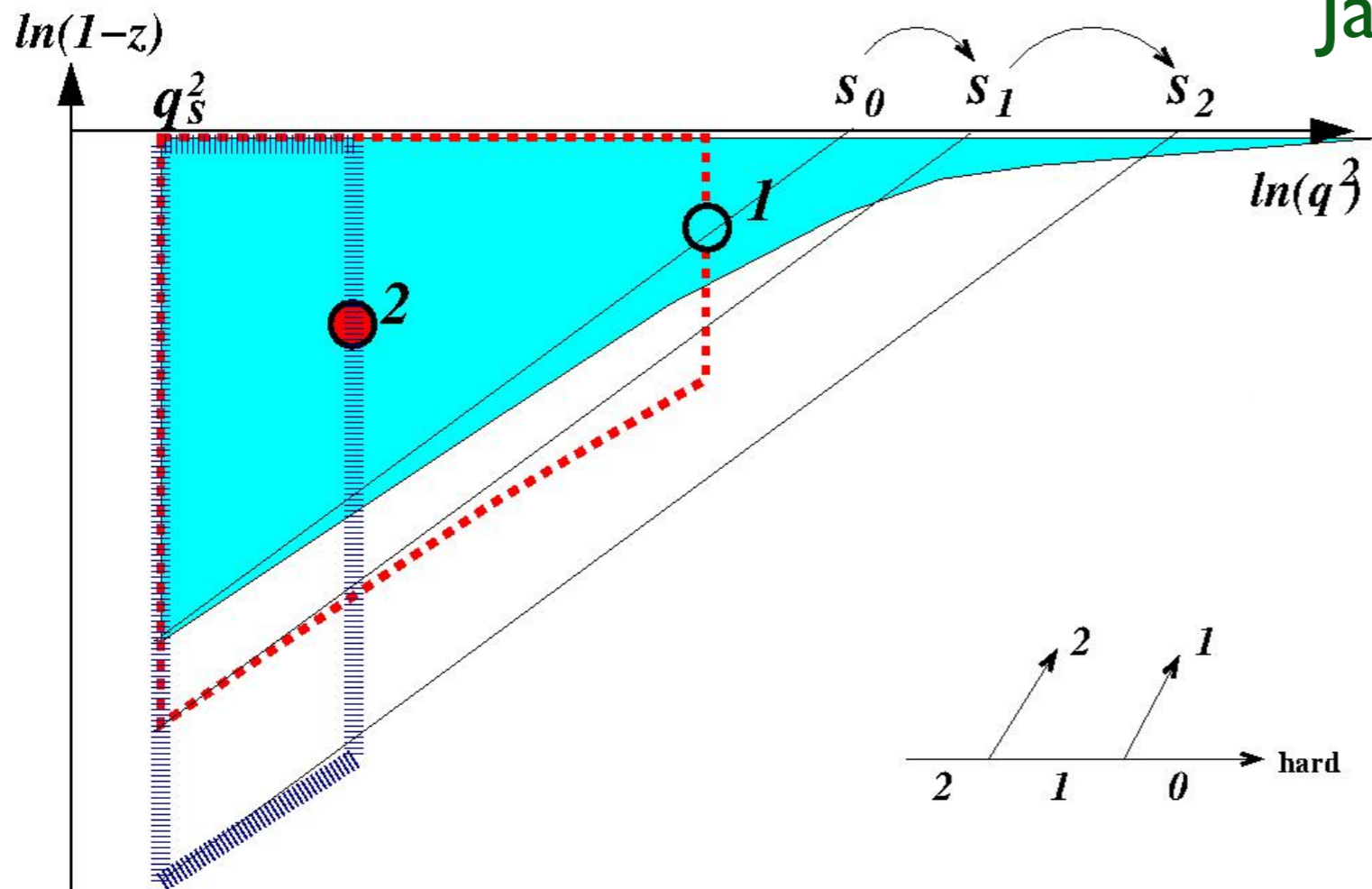


Deductor MC@NLO



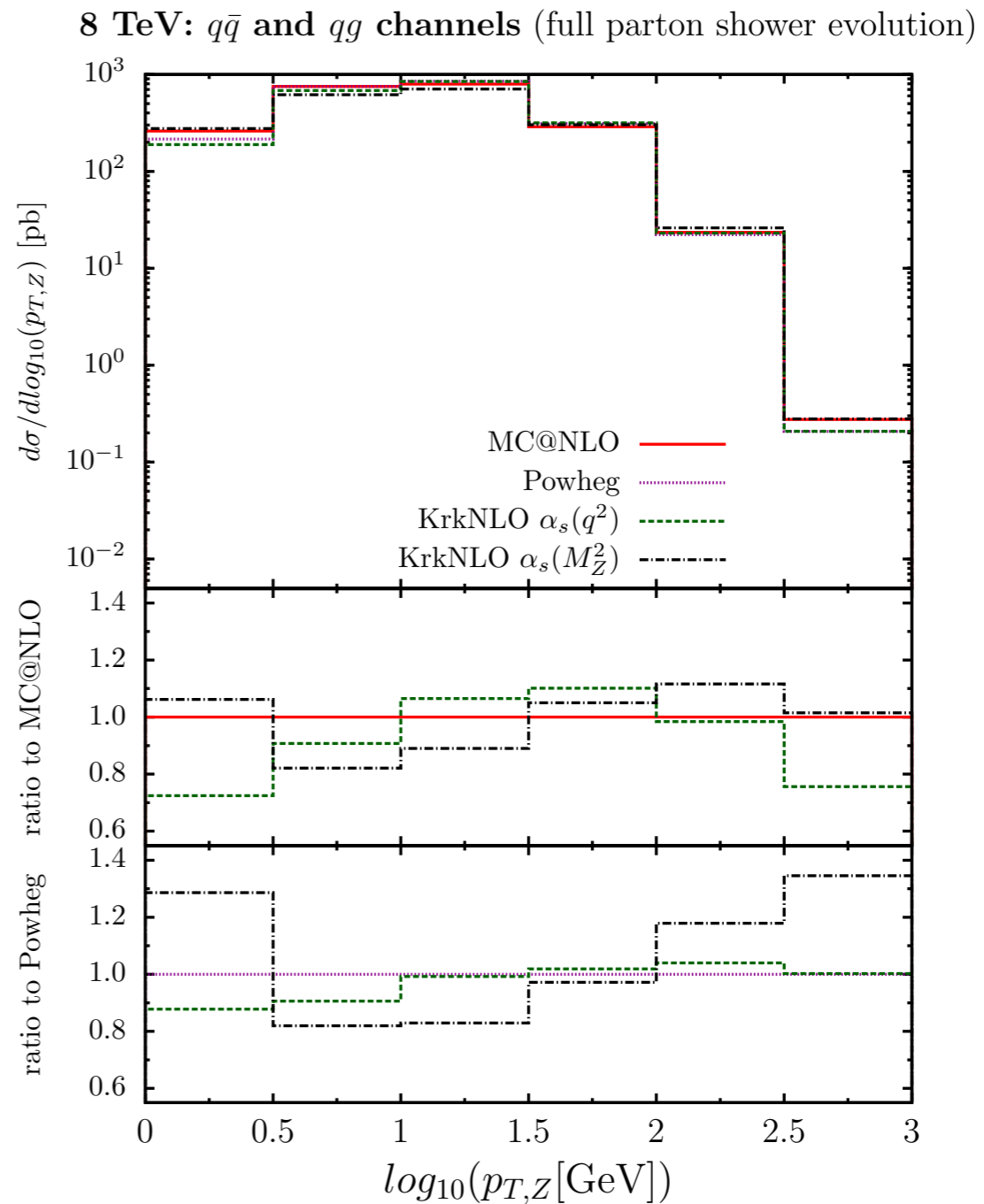
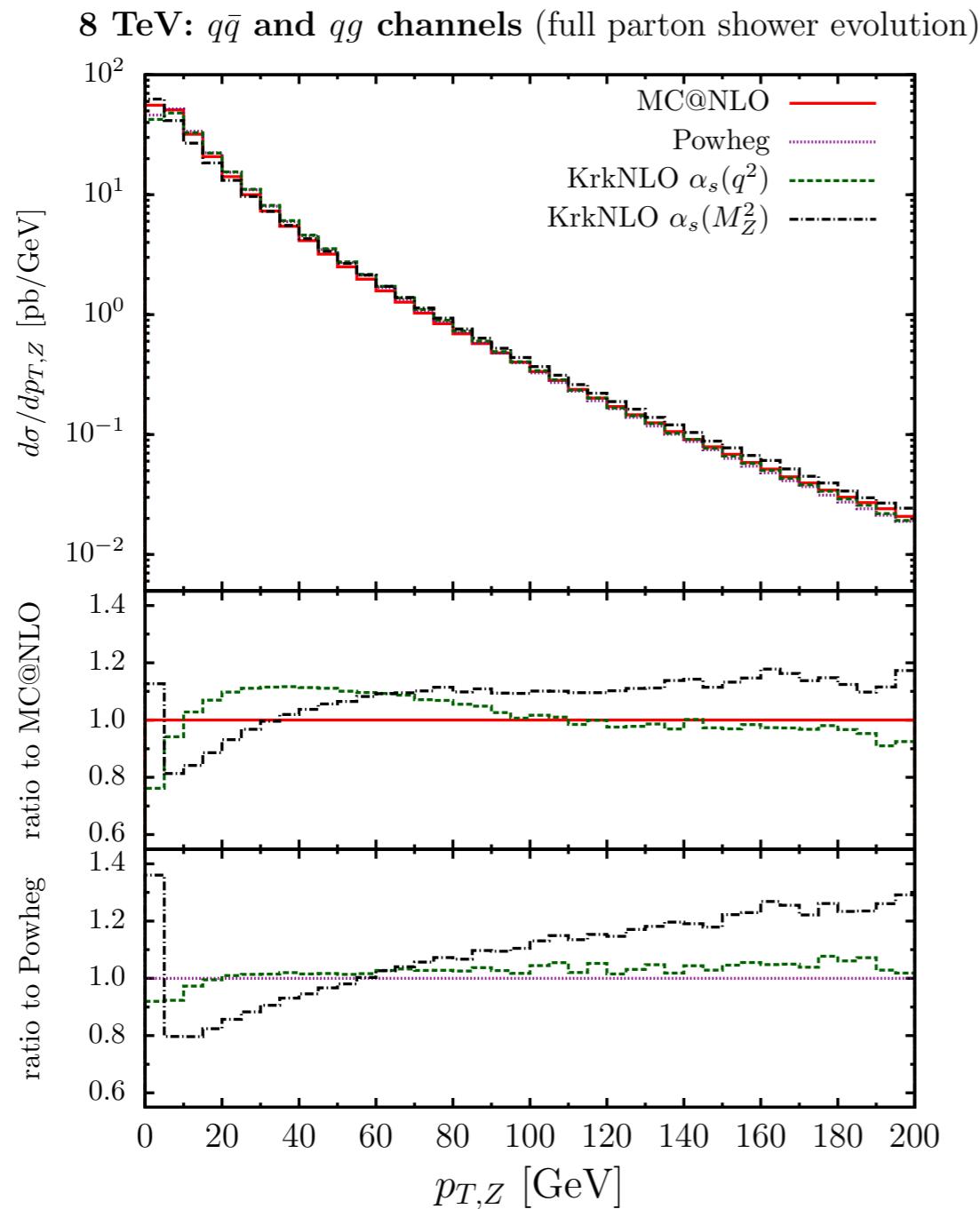
KrkNLO method

Jadach et al., 1503.06849



- Modified LO PS and PDF for full phase space
- NLO correction by multiplicative weight

KrkNLO results



- α_s choice is for first emission

Automatic NLO matching

- MC@NLO-type

- ✦ MadGraph5_aMC@NLO (MadLoop5)

Alwall et al., 1405.0301

- ✦ Sherpa+OpenLoops

Höche et al., 1111.1220; 1201.5882

- ✦ Herwig++ Matchbox+OpenLoops/GoSam

Plätzer, Gieseke, 1109.6256; Bellm et al., 1310.6877

- POWHEG-type

- ✦ MadGraph4+POWHEG+MCFM/GoSam

Campbell et al., 1202.5475; Luisoni et al., 1502.01213

- ✦ Herwig++ Matchbox+OpenLoops/GoSam

MG5_aMC@NLO

Process	Syntax	Cross section (pb)					
		LO 13 TeV			NLO 13 TeV		
Heavy quarks+vector bosons							
e.1	$pp \rightarrow W^\pm b\bar{b}$ (4f)	p p > wpm b b~	$3.074 \pm 0.002 \cdot 10^2$	+42.3% +2.0%	$8.162 \pm 0.034 \cdot 10^2$	+29.8% +1.5%	
e.2	$pp \rightarrow Z b\bar{b}$ (4f)	p p > z b b~	$6.993 \pm 0.003 \cdot 10^2$	-29.2% -1.6%	$1.235 \pm 0.004 \cdot 10^3$	-23.6% -1.2%	
e.3	$pp \rightarrow \gamma b\bar{b}$ (4f)	p p > a b b~	$1.731 \pm 0.001 \cdot 10^3$	+33.5% +1.0%	$4.171 \pm 0.015 \cdot 10^3$	+19.9% +1.0%	
e.4*	$pp \rightarrow W^\pm b\bar{b}j$ (4f)	p p > wpm b b~ j	$1.861 \pm 0.003 \cdot 10^2$	-24.4% -1.4%	$3.957 \pm 0.013 \cdot 10^2$	-17.4% -1.4%	
e.5*	$pp \rightarrow Z b\bar{b}j$ (4f)	p p > z b b~ j	$1.604 \pm 0.001 \cdot 10^2$	+51.9% +1.6%	$2.805 \pm 0.009 \cdot 10^2$	+33.7% +1.4%	
e.6*	$pp \rightarrow \gamma b\bar{b}j$ (4f)	p p > a b b~ j	$7.812 \pm 0.017 \cdot 10^2$	-34.8% -2.1%	$1.233 \pm 0.004 \cdot 10^3$	-27.1% -1.9%	
e.7	$pp \rightarrow t\bar{t}W^\pm$	p p > t t~ wpm	$3.777 \pm 0.003 \cdot 10^{-1}$	+42.5% +0.7%	$5.662 \pm 0.021 \cdot 10^{-1}$	+27.0% +0.7%	
e.8	$pp \rightarrow t\bar{t}Z$	p p > t t~ z	$5.273 \pm 0.004 \cdot 10^{-1}$	-27.7% -0.7%	$7.598 \pm 0.026 \cdot 10^{-1}$	-21.0% -0.6%	
e.9	$pp \rightarrow t\bar{t}\gamma$	p p > t t~ a	$1.204 \pm 0.001 \cdot 10^0$	+42.4% +0.9%	$1.744 \pm 0.005 \cdot 10^0$	+21.0% +0.8%	
e.10*	$pp \rightarrow t\bar{t}W^\pm j$	p p > t t~ wpm j	$2.352 \pm 0.002 \cdot 10^{-1}$	-27.6% -1.1%	$3.404 \pm 0.011 \cdot 10^{-1}$	-17.6% -1.0%	
e.11*	$pp \rightarrow t\bar{t}Zj$	p p > t t~ z j	$3.953 \pm 0.004 \cdot 10^{-1}$	+51.2% +1.0%	$5.074 \pm 0.016 \cdot 10^{-1}$	+18.9% +1.0%	
e.12*	$pp \rightarrow t\bar{t}\gamma j$	p p > t t~ a j	$8.726 \pm 0.010 \cdot 10^{-1}$	-32.0% -1.5%	$1.135 \pm 0.004 \cdot 10^0$	-19.9% -1.5%	
e.13*	$pp \rightarrow t\bar{t}W^-W^+$ (4f)	p p > t t~ w+ w-	$6.675 \pm 0.006 \cdot 10^{-3}$	+23.9% +2.1%	$9.904 \pm 0.026 \cdot 10^{-3}$	+11.2% +1.7%	
e.14*	$pp \rightarrow t\bar{t}W^\pm Z$	p p > t t~ wpm z	$2.404 \pm 0.002 \cdot 10^{-3}$	-18.0% -1.6%	$3.525 \pm 0.010 \cdot 10^{-3}$	-10.6% -1.3%	
e.15*	$pp \rightarrow t\bar{t}W^\pm\gamma$	p p > t t~ wpm a	$2.718 \pm 0.003 \cdot 10^{-3}$	+30.5% +1.8%	$3.927 \pm 0.013 \cdot 10^{-3}$	+9.7% +1.9%	
e.16*	$pp \rightarrow t\bar{t}ZZ$	p p > t t~ z z	$1.349 \pm 0.014 \cdot 10^{-3}$	-21.8% -2.1%	$1.840 \pm 0.007 \cdot 10^{-3}$	-11.1% -2.2%	
e.17*	$pp \rightarrow t\bar{t}Z\gamma$	p p > t t~ z a	$2.548 \pm 0.003 \cdot 10^{-3}$	+29.6% +1.6%	$3.656 \pm 0.012 \cdot 10^{-3}$	+9.8% +1.7%	
e.18*	$pp \rightarrow t\bar{t}\gamma\gamma$	p p > t t~ a a	$3.272 \pm 0.006 \cdot 10^{-3}$	-21.3% -1.8%	$4.402 \pm 0.015 \cdot 10^{-3}$	-11.0% -2.0%	

- Sampled from 172 processes
- Mostly new at NLO

Alwall et al., 1405.0301

MG5_aMC@NLO

Process	Syntax	Cross section (pb)				
		LO 1 TeV		NLO 1 TeV		
j.1	$e^+e^- \rightarrow t\bar{t}H$	e+ e- > t t~ h	$2.018 \pm 0.003 \cdot 10^{-3}$	+0.0% -0.0%	$1.911 \pm 0.006 \cdot 10^{-3}$	+0.4% -0.5%
j.2*	$e^+e^- \rightarrow t\bar{t}Hj$	e+ e- > t t~ h j	$2.533 \pm 0.003 \cdot 10^{-4}$	+9.2% -7.8%	$2.658 \pm 0.009 \cdot 10^{-4}$	+0.5% -1.5%
j.3*	$e^+e^- \rightarrow t\bar{t}Hjj$	e+ e- > t t~ h j j	$2.663 \pm 0.004 \cdot 10^{-5}$	+19.3% -14.9%	$3.278 \pm 0.017 \cdot 10^{-5}$	+4.0% -5.7%
j.4*	$e^+e^- \rightarrow t\bar{t}\gamma$	e+ e- > t t~ a	$1.270 \pm 0.002 \cdot 10^{-2}$	+0.0% -0.0%	$1.335 \pm 0.004 \cdot 10^{-2}$	+0.5% -0.4%
j.5*	$e^+e^- \rightarrow t\bar{t}\gamma j$	e+ e- > t t~ a j	$2.355 \pm 0.002 \cdot 10^{-3}$	+9.3% -7.9%	$2.617 \pm 0.010 \cdot 10^{-3}$	+1.6% -2.4%
j.6*	$e^+e^- \rightarrow t\bar{t}\gamma jj$	e+ e- > t t~ a j j	$3.103 \pm 0.005 \cdot 10^{-4}$	+19.5% -15.0%	$4.002 \pm 0.021 \cdot 10^{-4}$	+5.4% -6.6%
j.7*	$e^+e^- \rightarrow t\bar{t}Z$	e+ e- > t t~ z	$4.642 \pm 0.006 \cdot 10^{-3}$	+0.0% -0.0%	$4.949 \pm 0.014 \cdot 10^{-3}$	+0.6% -0.5%
j.8*	$e^+e^- \rightarrow t\bar{t}Zj$	e+ e- > t t~ z j	$6.059 \pm 0.006 \cdot 10^{-4}$	+9.3% -7.8%	$6.940 \pm 0.028 \cdot 10^{-4}$	+2.0% -2.6%
j.9*	$e^+e^- \rightarrow t\bar{t}Zjj$	e+ e- > t t~ z j j	$6.351 \pm 0.028 \cdot 10^{-5}$	+19.4% -15.0%	$8.439 \pm 0.051 \cdot 10^{-5}$	+5.8% -6.8%
j.10*	$e^+e^- \rightarrow t\bar{t}W^\pm jj$	e+ e- > t t~ wpm j j	$2.400 \pm 0.004 \cdot 10^{-7}$	+19.3% -14.9%	$3.723 \pm 0.012 \cdot 10^{-7}$	+9.6% -9.1%
j.11*	$e^+e^- \rightarrow t\bar{t}HZ$	e+ e- > t t~ h z	$3.600 \pm 0.006 \cdot 10^{-5}$	+0.0% -0.0%	$3.579 \pm 0.013 \cdot 10^{-5}$	+0.1% -0.0%
j.12*	$e^+e^- \rightarrow t\bar{t}\gamma Z$	e+ e- > t t~ a z	$2.212 \pm 0.003 \cdot 10^{-4}$	+0.0% -0.0%	$2.364 \pm 0.006 \cdot 10^{-4}$	+0.6% -0.5%
j.13*	$e^+e^- \rightarrow t\bar{t}\gamma H$	e+ e- > t t~ a h	$9.756 \pm 0.016 \cdot 10^{-5}$	+0.0% -0.0%	$9.423 \pm 0.032 \cdot 10^{-5}$	+0.3% -0.4%
j.14*	$e^+e^- \rightarrow t\bar{t}\gamma\gamma$	e+ e- > t t~ a a	$3.650 \pm 0.008 \cdot 10^{-4}$	+0.0% -0.0%	$3.833 \pm 0.013 \cdot 10^{-4}$	+0.4% -0.4%
j.15*	$e^+e^- \rightarrow t\bar{t}ZZ$	e+ e- > t t~ z z	$3.788 \pm 0.004 \cdot 10^{-5}$	+0.0% -0.0%	$4.007 \pm 0.013 \cdot 10^{-5}$	+0.5% -0.5%
j.16*	$e^+e^- \rightarrow t\bar{t}HH$	e+ e- > t t~ h h	$1.358 \pm 0.001 \cdot 10^{-5}$	+0.0% -0.0%	$1.206 \pm 0.003 \cdot 10^{-5}$	+0.9% -1.1%
j.17*	$e^+e^- \rightarrow t\bar{t}W^+W^-$	e+ e- > t t~ w+ w-	$1.372 \pm 0.003 \cdot 10^{-4}$	+0.0% -0.0%	$1.540 \pm 0.006 \cdot 10^{-4}$	+1.0% -0.9%

- All new at NLO except ttH

NNLO matching

NNLO matching

- Fully inclusive NNLO, one extra jet NLO
- So far, limited to DY, H

- ✦ MiNLO-NNLOPS

Hamilton et al., 1309.0017, 1407.3773

- ✦ UN²LOPS

Höche, Li, Prestel, 1405.3607, 1407.3773

- ✦ Geneva

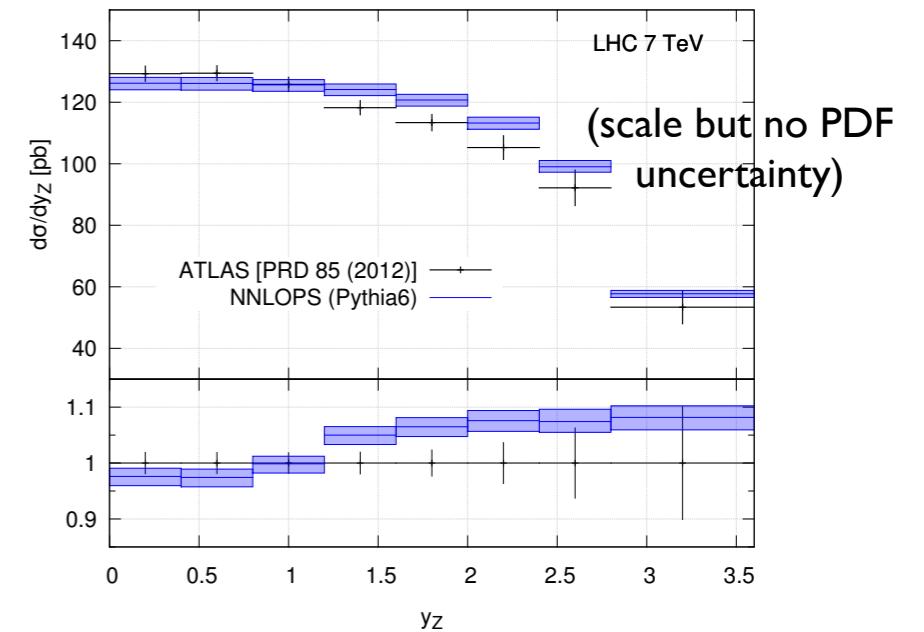
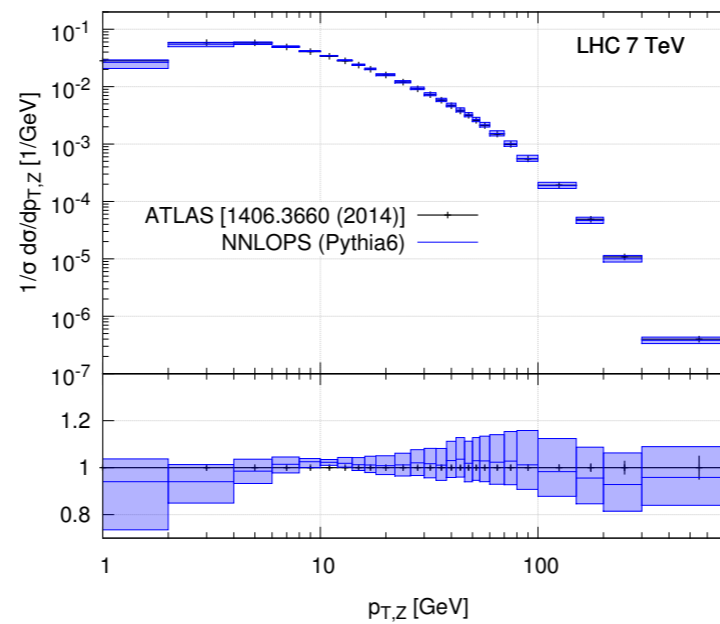
Alioli et al., 1311.0286

MiNLO-NNLOPS

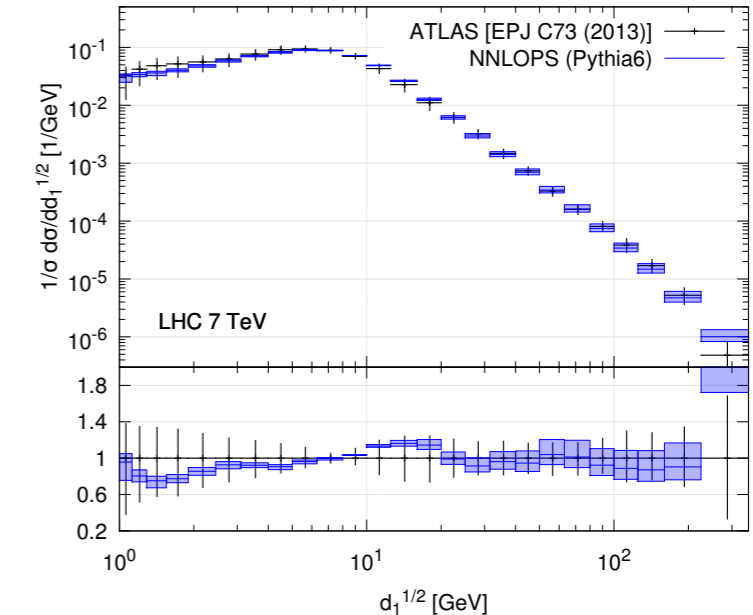
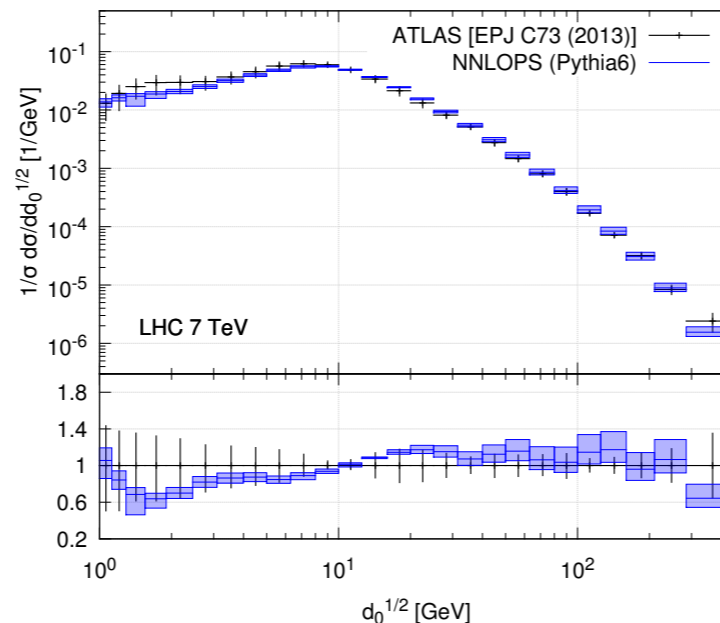
- Modified DY/H+jet POWHEG with NNLL Sudakov (B_2)
- Reweighted to NNLO

Karlberg, Re, Zanderighi, 1407.2940

- Z $p_{T,Z}$, rapidity



- W $d_{0,I}$ (k_t alg.)



UN²LOPS

Höche, Li, Prestel, I405.3607

- Phase space slicing at $q_T \sim 1 \text{ GeV}$ (DY, H)
- q_T subtraction: NNLO in zero bin
- extra jet at NLO

$$\begin{aligned} \langle O \rangle^{(\text{UN}^2\text{LOPS})} &= \int d\Phi_0 \bar{B}_0^{q_T, \text{cut}}(\Phi_0) O(\Phi_0) \\ &+ \int_{q_T, \text{cut}} d\Phi_1 \left[1 - \Pi_0(t_1, \mu_Q^2) \left(w_1(\Phi_1) + w_1^{(1)}(\Phi_1) + \Pi_0^{(1)}(t_1, \mu_Q^2) \right) \right] B_1(\Phi_1) O(\Phi_0) \\ &+ \int_{q_T, \text{cut}} d\Phi_1 \Pi_0(t_1, \mu_Q^2) \left(w_1(\Phi_1) + w_1^{(1)}(\Phi_1) + \Pi_0^{(1)}(t_1, \mu_Q^2) \right) B_1(\Phi_1) \bar{\mathcal{F}}_1(t_1, O) \\ &+ \int_{q_T, \text{cut}} d\Phi_1 \left[1 - \Pi_0(t_1, \mu_Q^2) \right] \tilde{B}_1^{\text{R}}(\Phi_1) O(\Phi_0) + \int_{q_T, \text{cut}} d\Phi_1 \Pi_0(t_1, \mu_Q^2) \tilde{B}_1^{\text{R}}(\Phi_1) \bar{\mathcal{F}}_1(t_1, O) \\ &+ \int_{q_T, \text{cut}} d\Phi_2 \left[1 - \Pi_0(t_1, \mu_Q^2) \right] H_1^{\text{R}}(\Phi_2) O(\Phi_0) + \int_{q_T, \text{cut}} d\Phi_2 \Pi_0(t_1, \mu_Q^2) H_1^{\text{R}}(\Phi_2) \mathcal{F}_2(t_2, O) \\ &+ \int_{q_T, \text{cut}} d\Phi_2 H_1^{\text{E}}(\Phi_2) \mathcal{F}_2(t_2, O) \end{aligned}$$

UN²LOPS results (DY)

Höche, Li, Prestel, 1405.3607

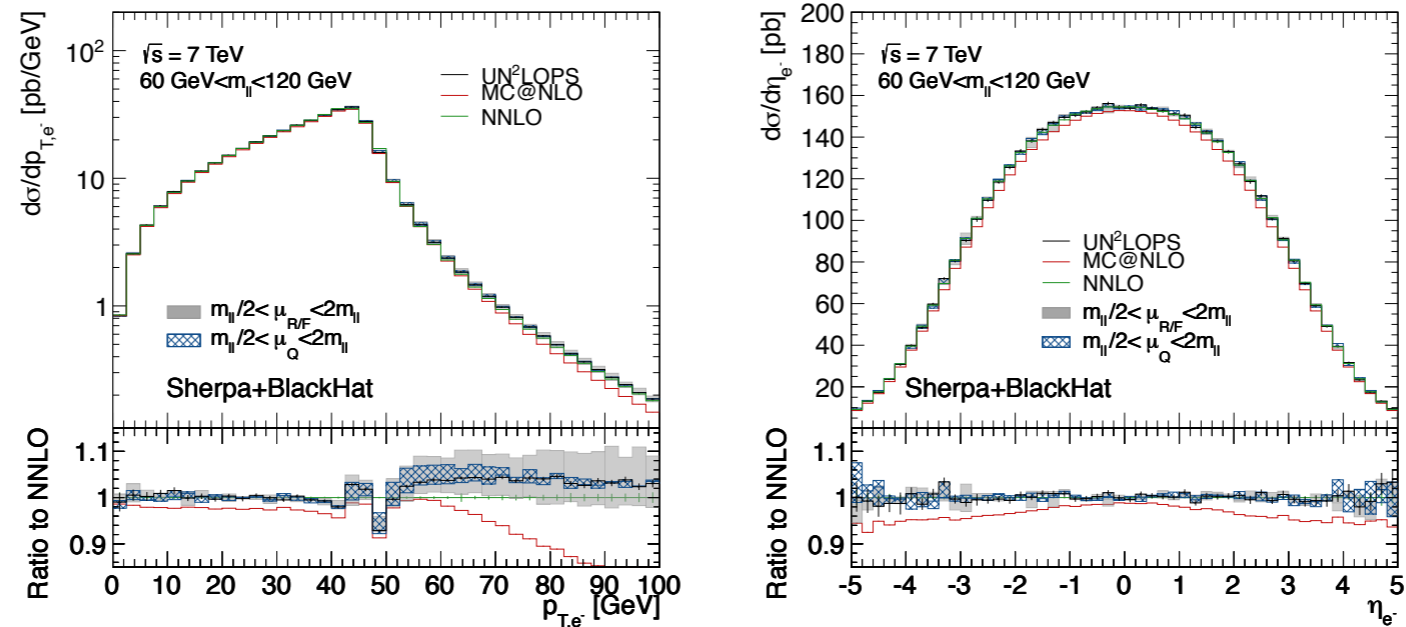


FIG. 2. Transverse momentum and rapidity spectrum of the electron. The gray solid (blue hatched) band shows scale uncertainties obtained by varying $\mu_{R/F}$ (μ_Q) in the range $m_U/2 \leq \mu \leq 2m_U$.

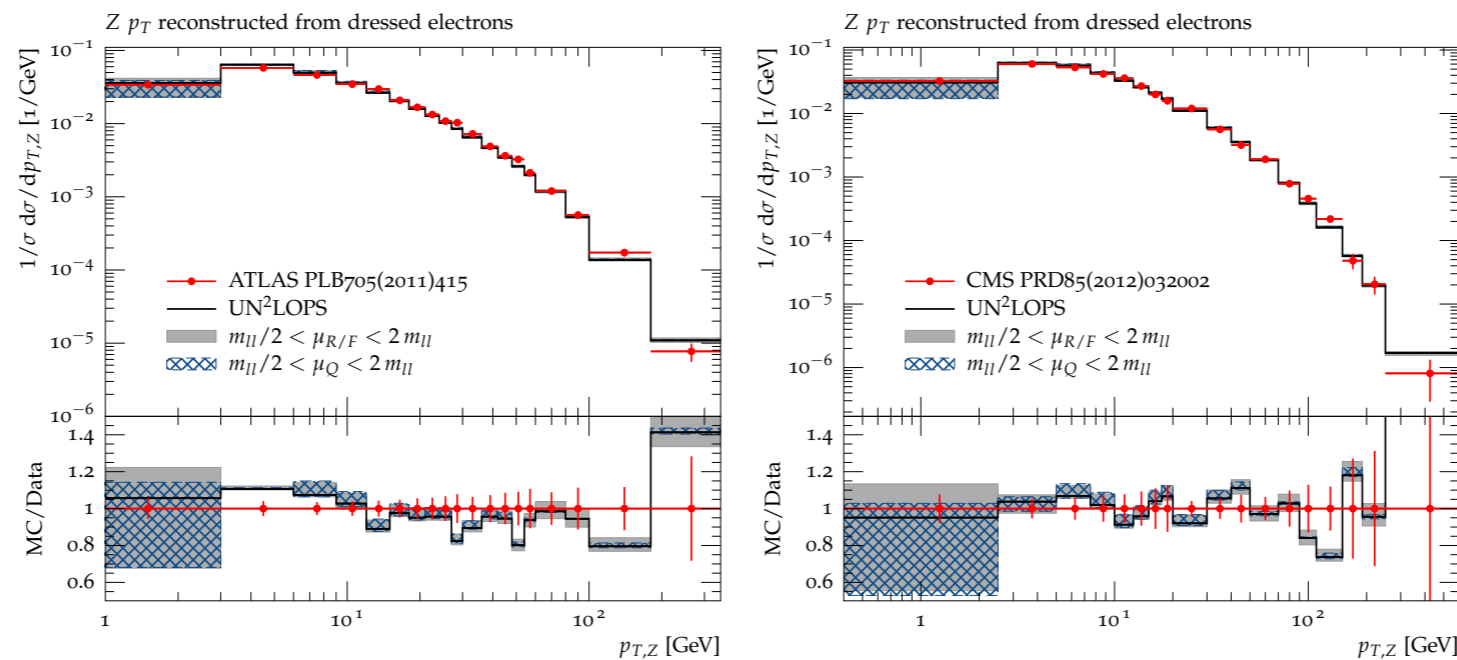


FIG. 3. UN²LOPS prediction for the transverse momentum spectrum of the Drell-Yan lepton pair in comparison to ATLAS data from [39] (left) and CMS data from [38] (right). The gray solid (blue hatched) band shows scale uncertainties obtained by varying $\mu_{R/F}$ (μ_Q) in the range $m_U/2 \leq \mu \leq 2m_U$.

UN²LOPS results (Higgs)

Höche, Li, Prestel, 1407.3773

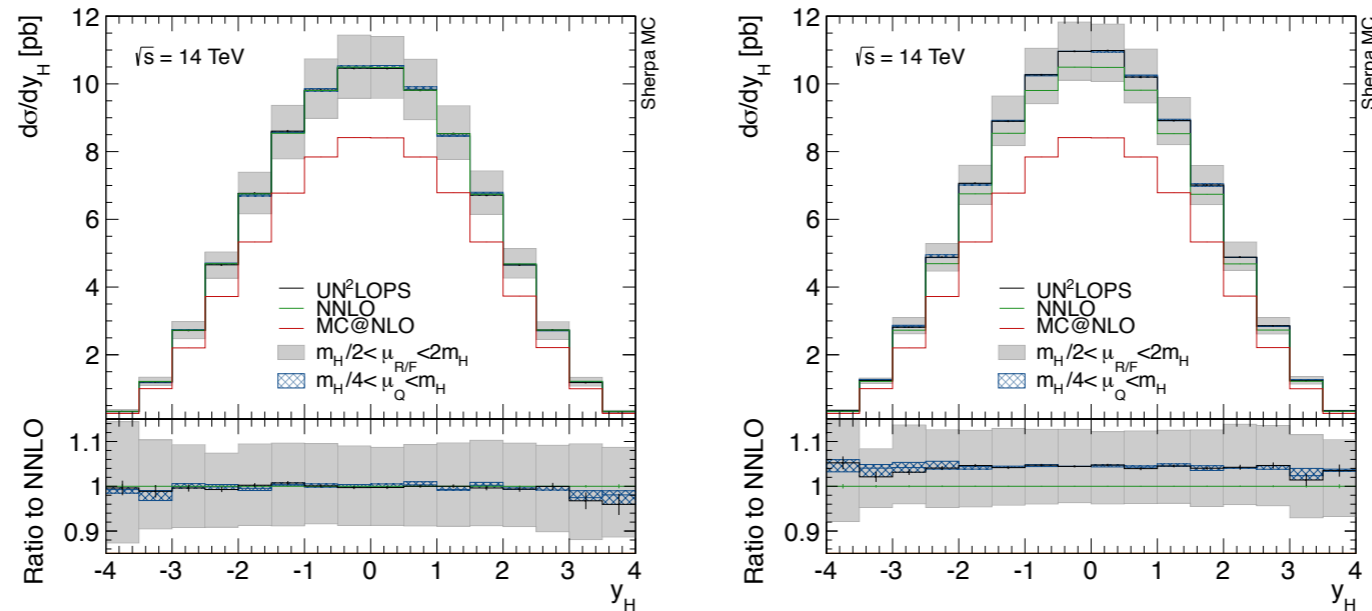


FIG. 2. Rapidity spectrum of the Higgs boson in individual matching (left) and factorized matching (right). See Sec. IV for details.

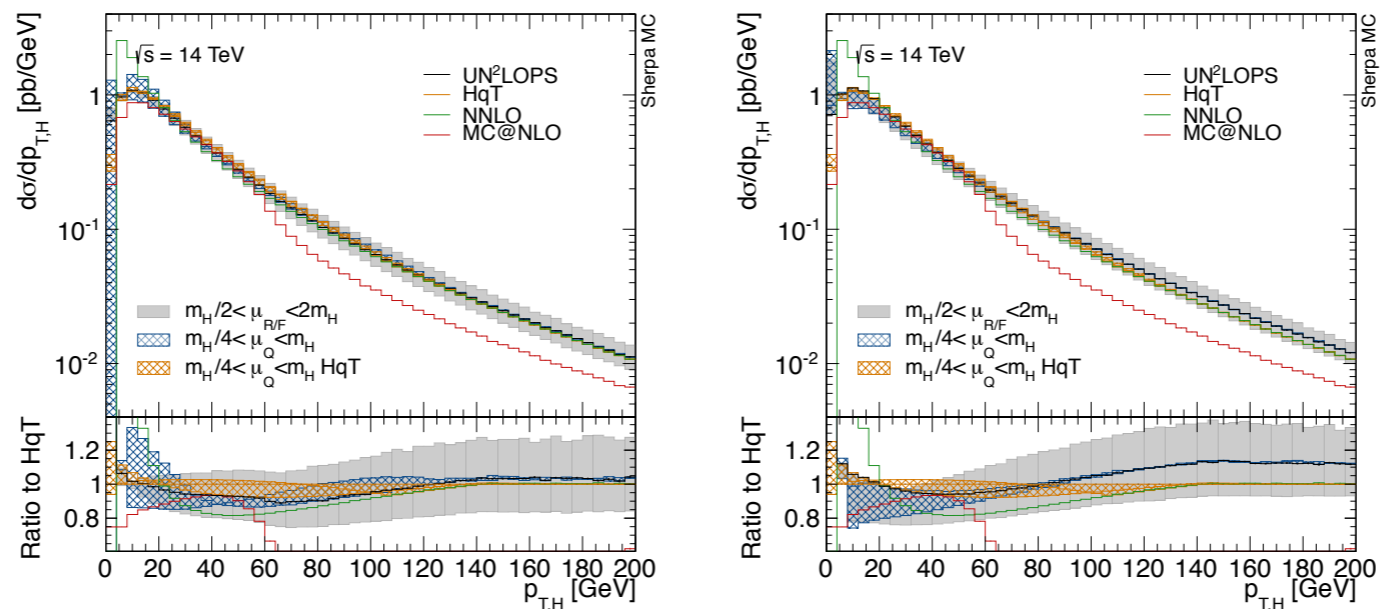


FIG. 3. Transverse momentum spectrum of the Higgs boson in individual matching (left) and factorized matching (right). See Sec. IV for details.

Matching to multiple fixed orders

Merging at NLO (?)

- Separate samples by jet resolution, e.g. d_{cut}
- Make NLO for $d_{i+1} < d_{\text{cut}} < d_i$
- Avoid double counting
- Reduce d_{cut} dependence
- ❖ MEPS@NLO: Höche et al., 1207.5030
- ❖ FxFx: Frederix, Frixione, 1209.6215
- ❖ Geneva: Alioli et al., 1211.7049
- ❖ UNLOPS: Lönnblad, Prestel, 1211.7278, Plätzer, 1211.5467

MEPS@NLO

- $W+0,1,2$ jets at NLO
- $W+3,4$ jets at LO

Höche et al., 1207.5030

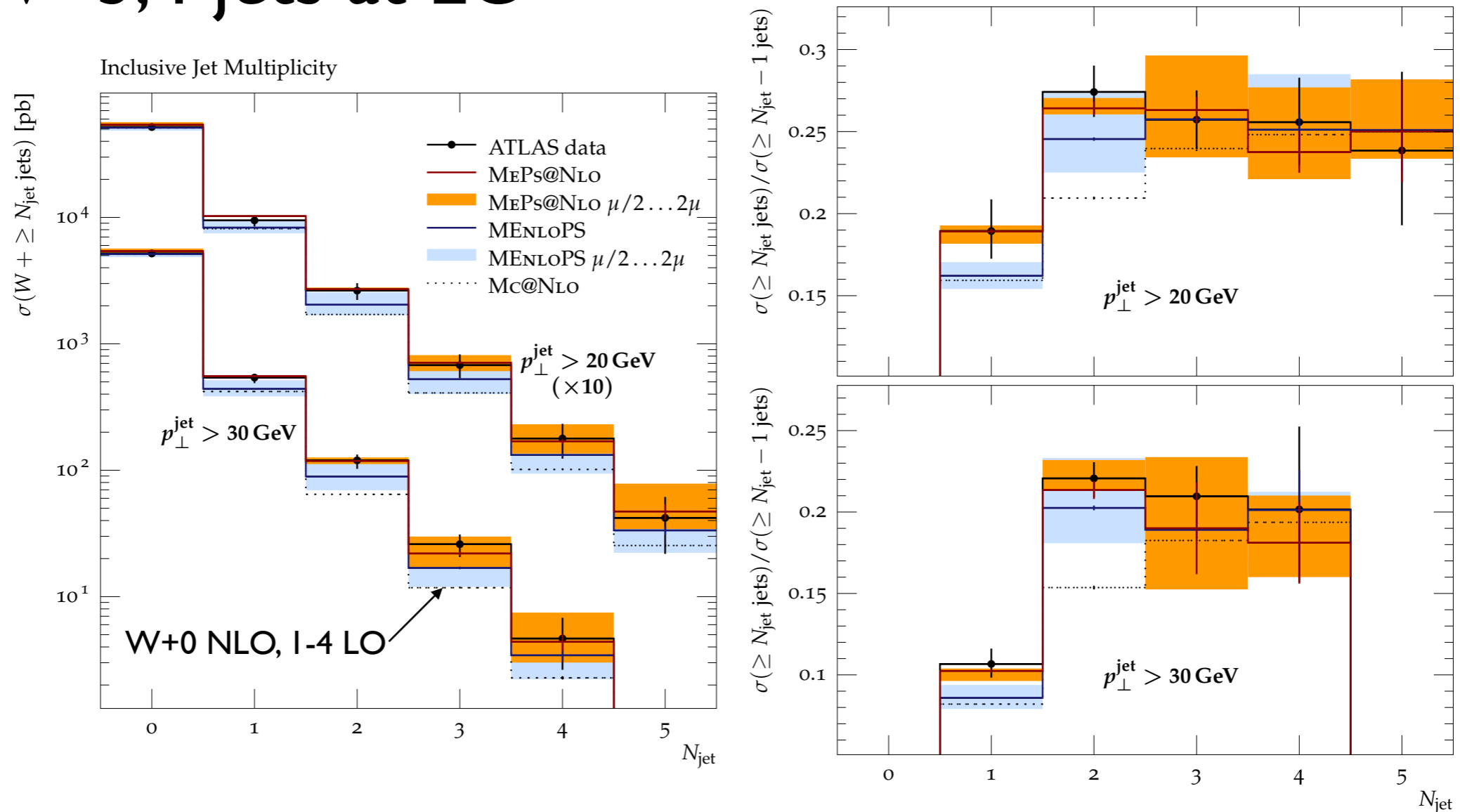


Figure 1: Cross section as a function of the inclusive jet multiplicity (left) and their ratios (right) in W +jets events measured by ATLAS [50].

FxFx merging

Frederix, Frixione, I209.6215

- \mathbb{S} and \mathbb{H} event samples for each multiplicity ($D(d_i) \approx \Theta(\mu_2 - d_i)$)

$$d\bar{\sigma}_{\mathbb{S},0} = T_0 + V_0 - T_0\mathcal{K} + T_0\mathcal{K}_{\text{MC}}D(d_1(\Xi_{\mathbb{H},0})),$$

$$d\bar{\sigma}_{\mathbb{H},0} = \left[T_1 - T_0\mathcal{K}_{\text{MC}} \right] D(d_1(\Xi_{\mathbb{H},0})),$$

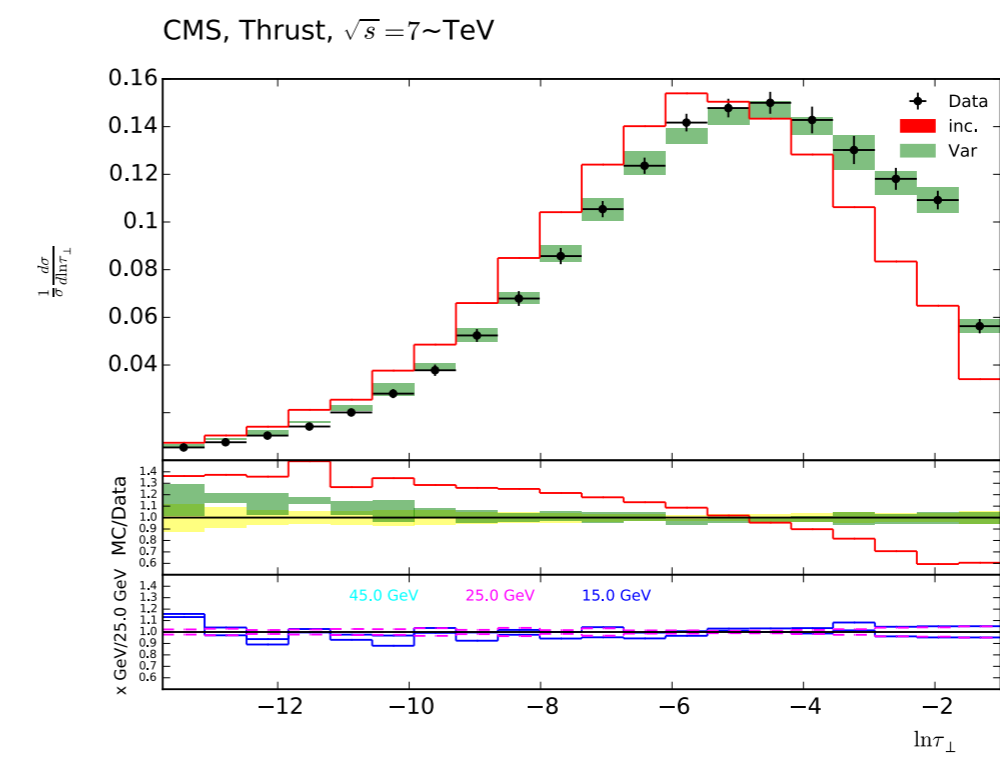
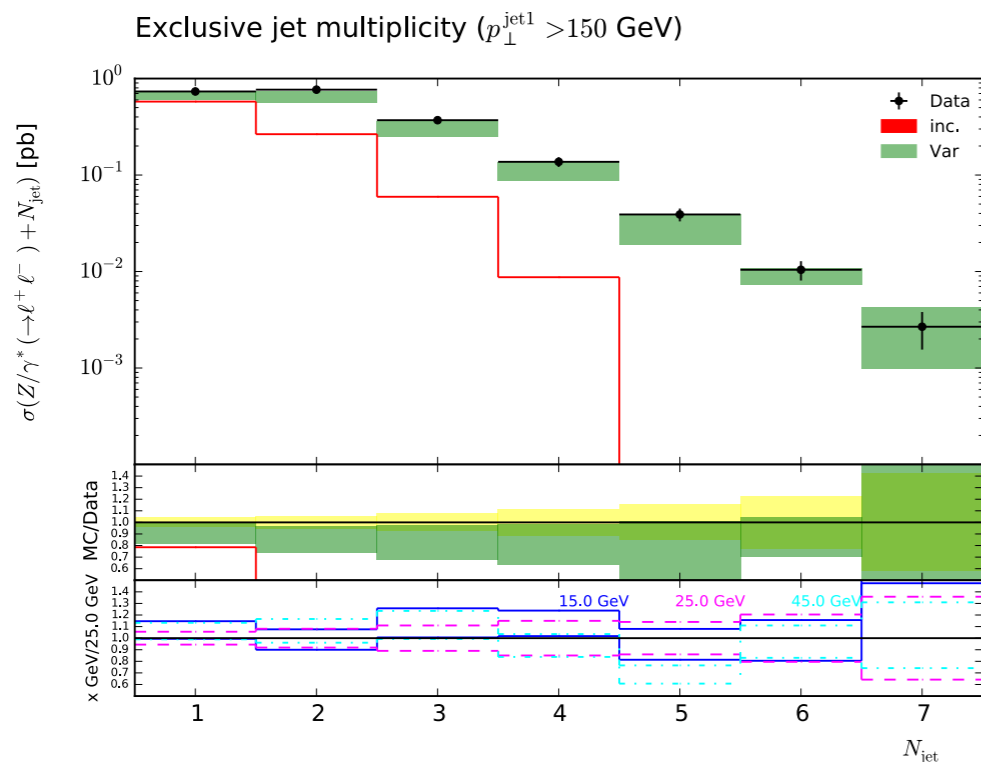
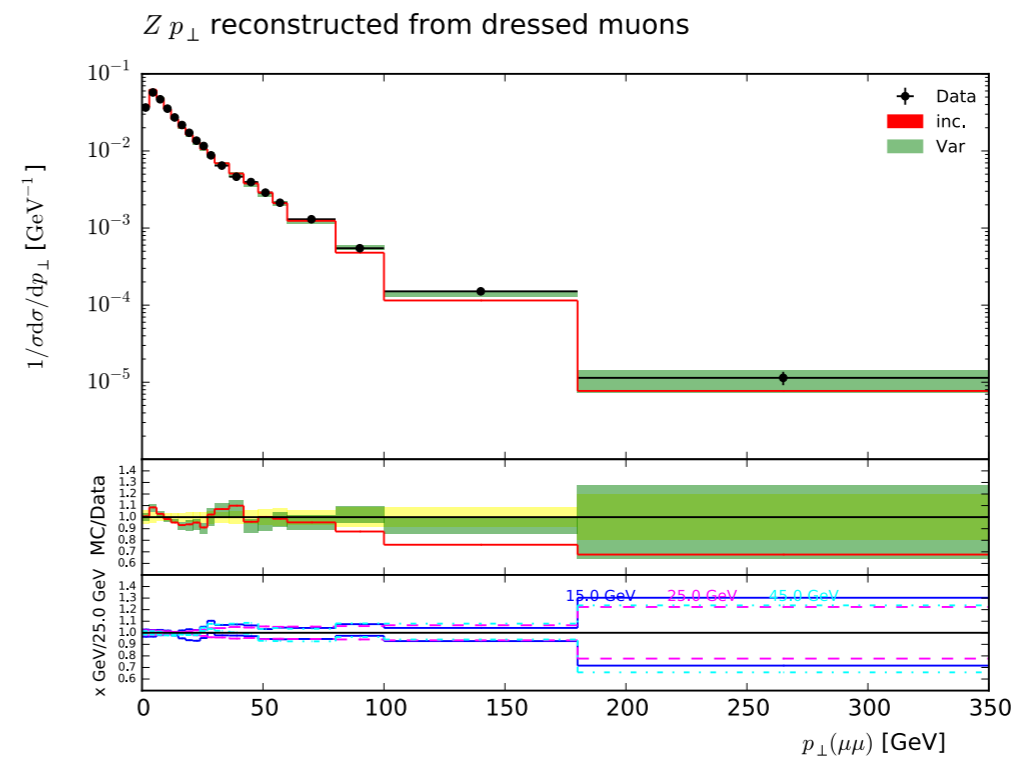
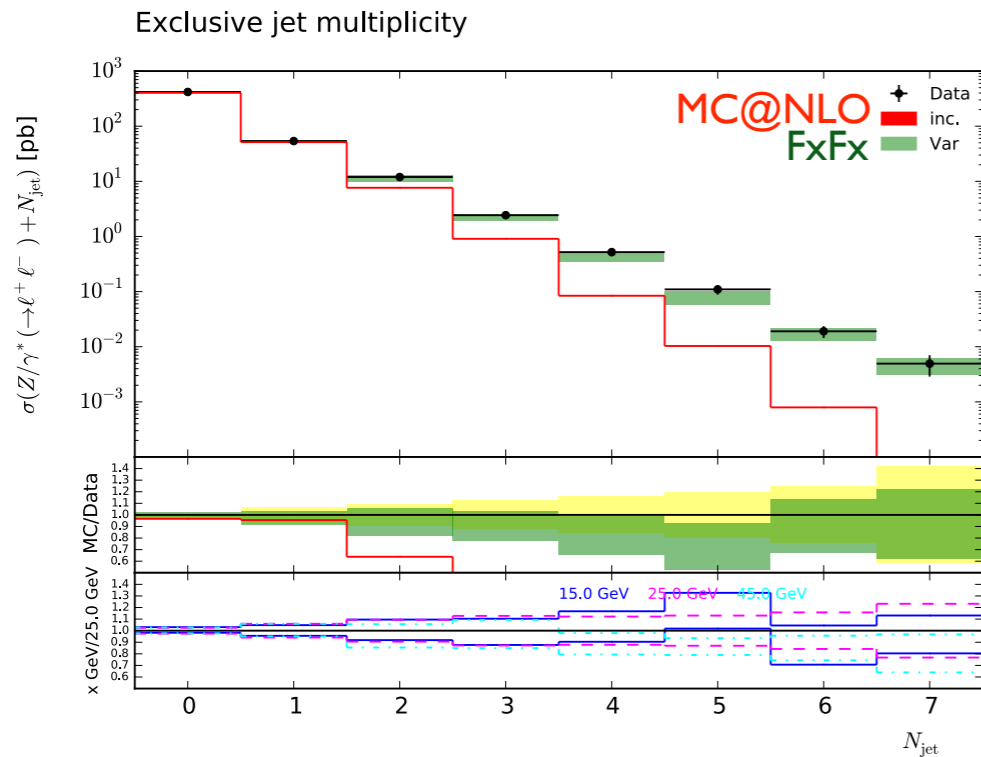
$$d\bar{\sigma}_{\mathbb{S},i} = \left[T_i + V_i - T_i\mathcal{K} + T_i\mathcal{K}_{\text{MC}}D(d_{i+1}(\Xi_{\mathbb{H},i})) \right] \\ \times (1 - D(d_i(\Xi_{\mathbb{S},i}))) \Theta(d_{i-1}(\Xi_{\mathbb{S},i}) - \mu_2),$$

$$d\bar{\sigma}_{\mathbb{H},i} = \left[T_{i+1} (1 - D(d_i(\Xi_{\mathbb{H},i}))) \Theta(d_{i-1}(\Xi_{\mathbb{H},i}) - \mu_2) \right. \\ \left. - T_i\mathcal{K}_{\text{MC}} (1 - D(d_i(\Xi_{\mathbb{S},i}))) \Theta(d_{i-1}(\Xi_{\mathbb{S},i}) - \mu_2) \right] D(d_{i+1}(\Xi_{\mathbb{H},i})),$$

$$d\bar{\sigma}_{\mathbb{S},N} = \left[T_N + V_N - T_N\mathcal{K} + T_N\mathcal{K}_{\text{MC}} \right] \\ \times (1 - D(d_N(\Xi_{\mathbb{S},N}))) \Theta(d_{N-1}(\Xi_{\mathbb{S},N}) - \mu_2),$$

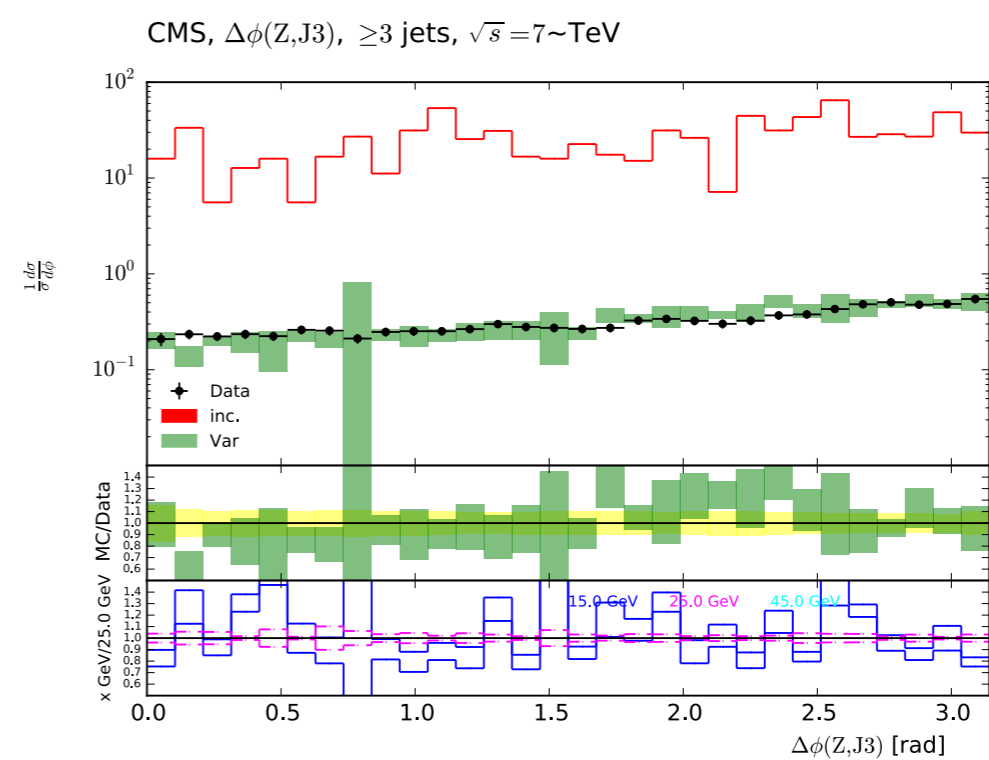
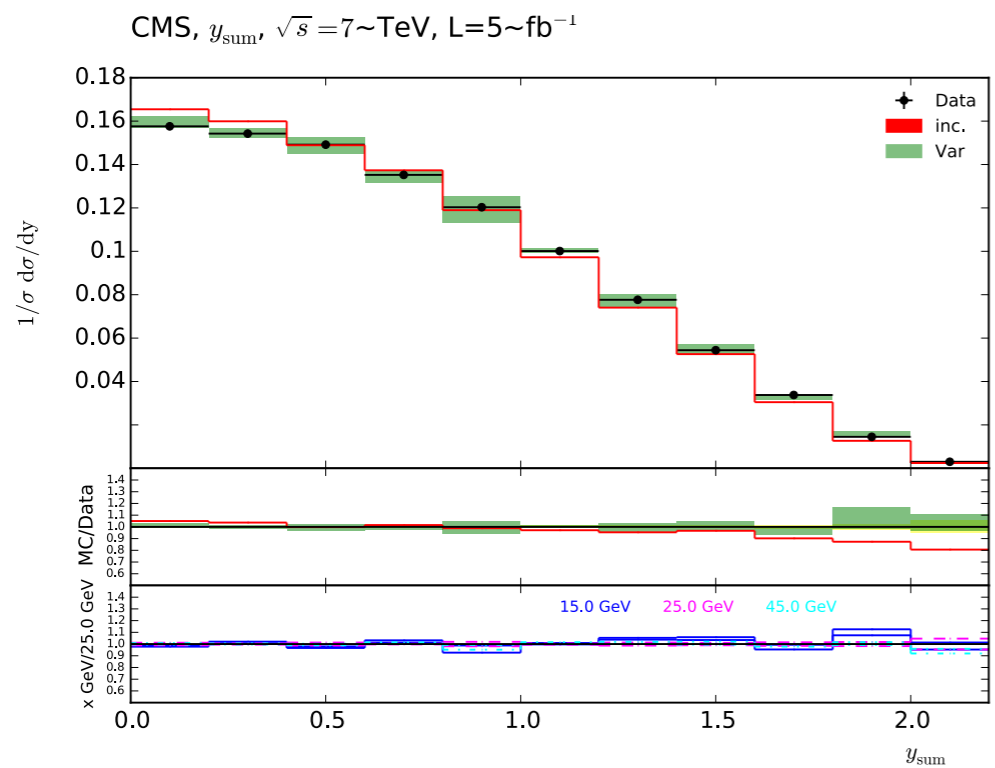
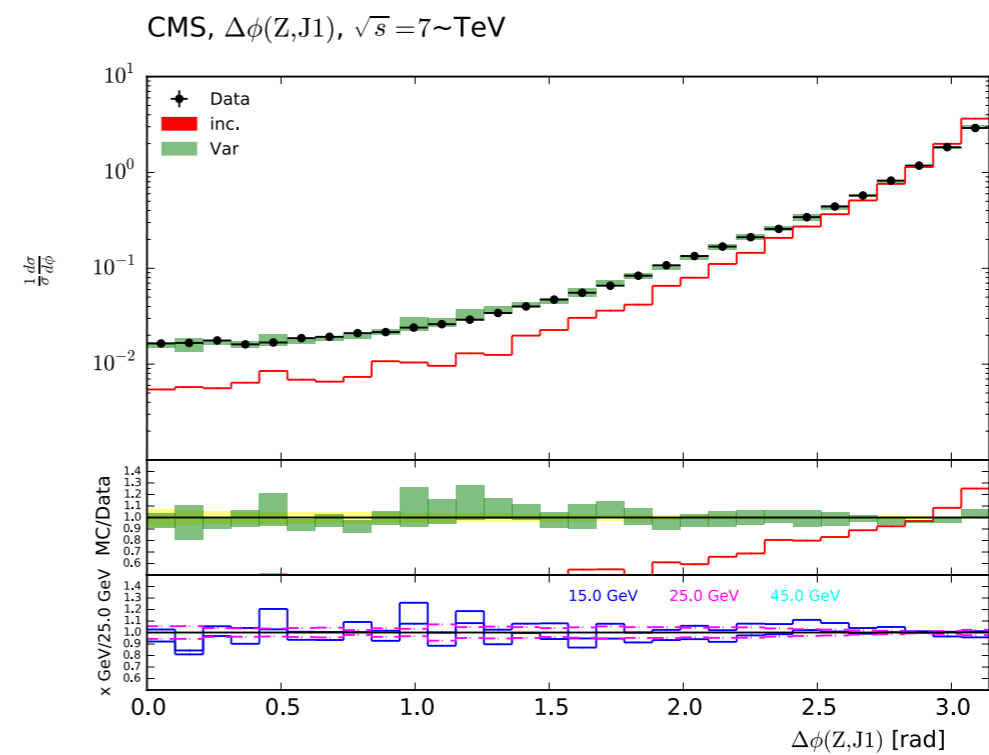
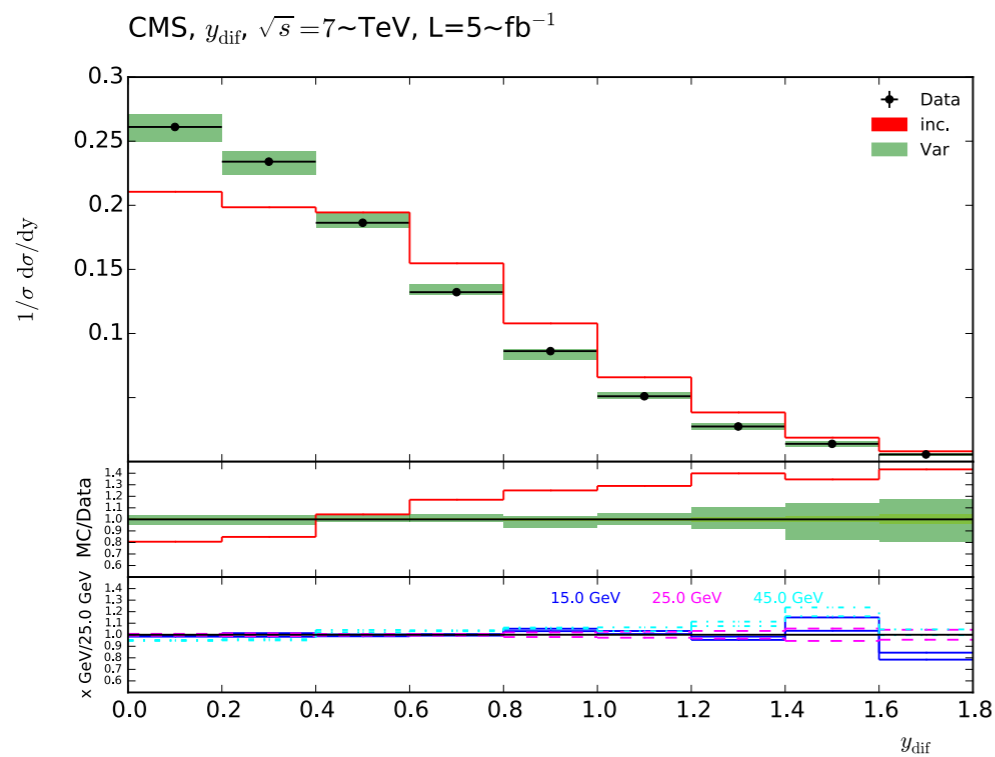
$$d\bar{\sigma}_{\mathbb{H},N} = T_{N+1} (1 - D(d_N(\Xi_{\mathbb{H},N}))) \Theta(d_{N-1}(\Xi_{\mathbb{H},N}) - \mu_2) \\ - T_N\mathcal{K}_{\text{MC}} (1 - D(d_N(\Xi_{\mathbb{S},N}))) \Theta(d_{N-1}(\Xi_{\mathbb{S},N}) - \mu_2).$$

FxFx Z results (I)

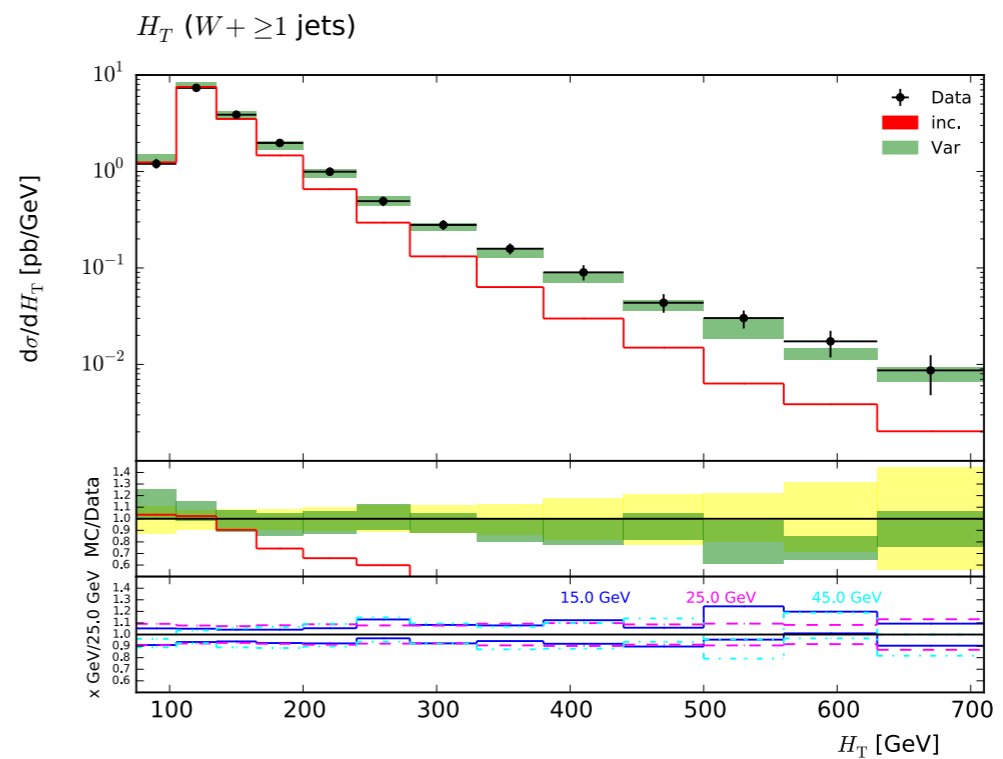
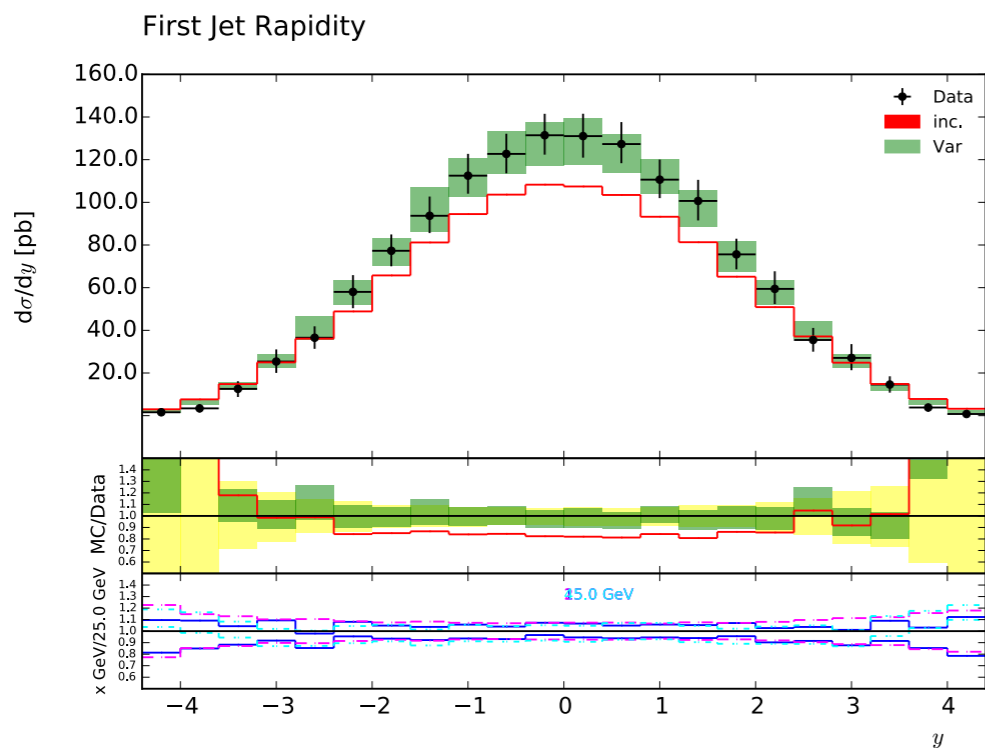
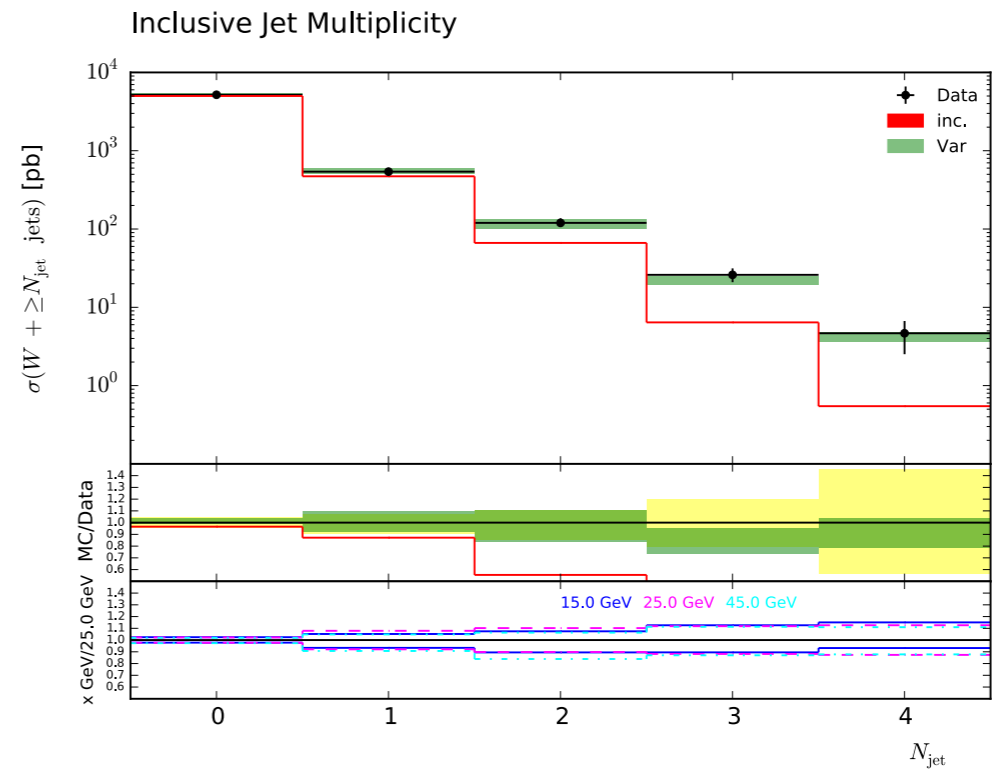
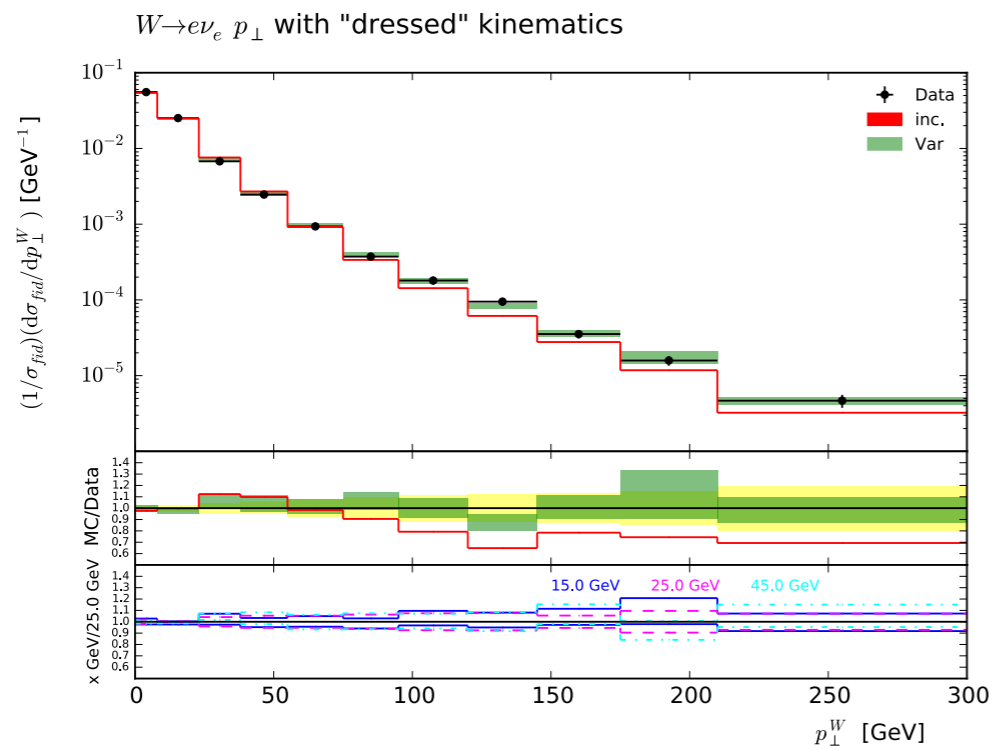


Frederix, Frixione, Papaefstathiou, Prestel, Torrielli, in prep.

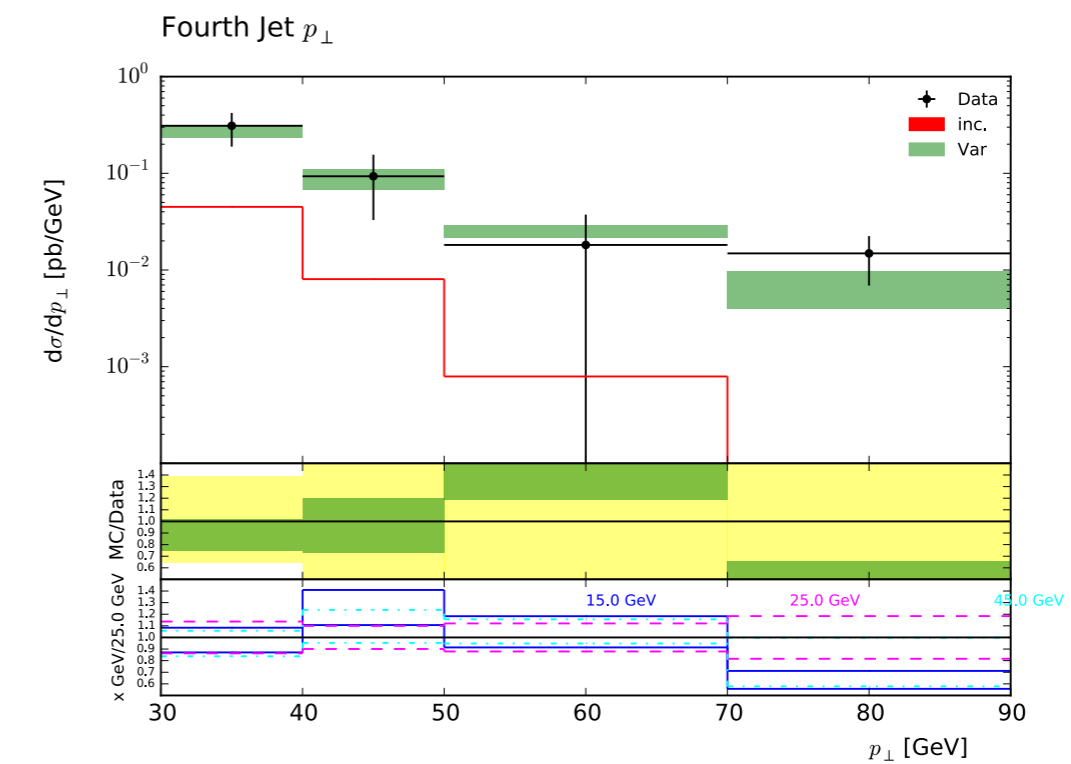
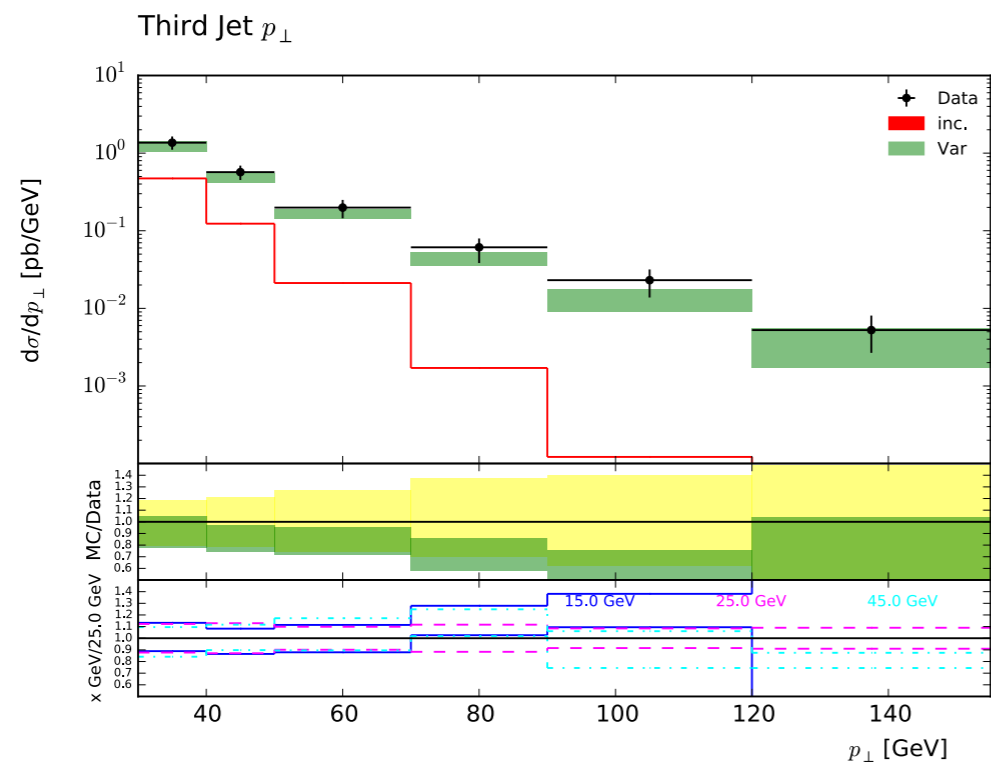
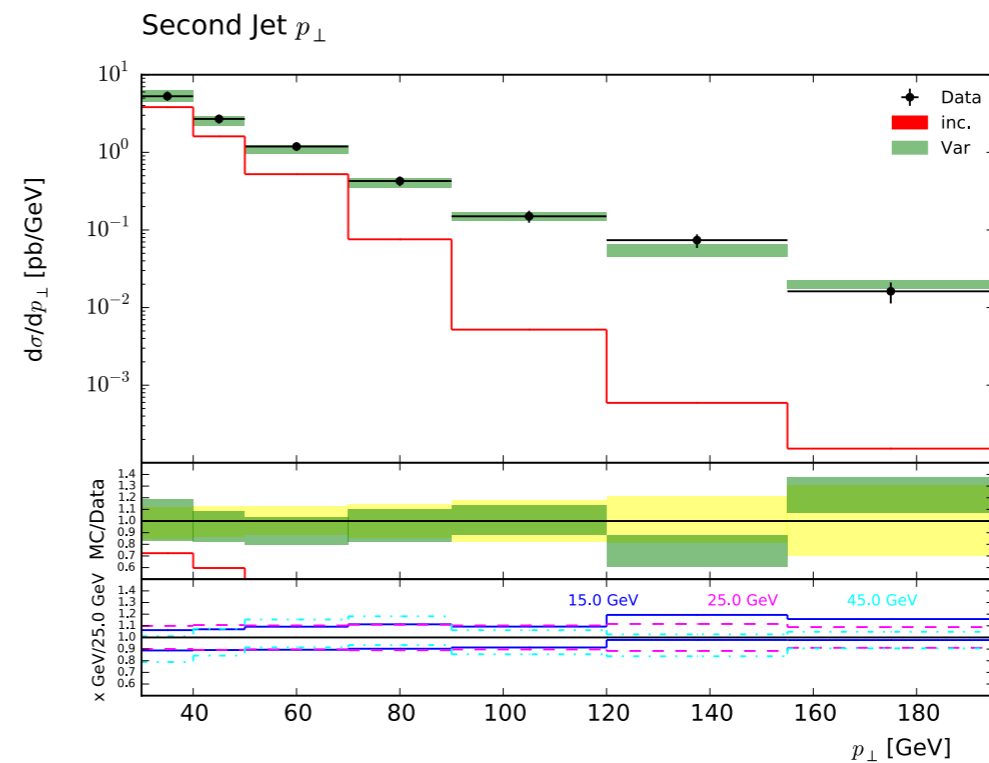
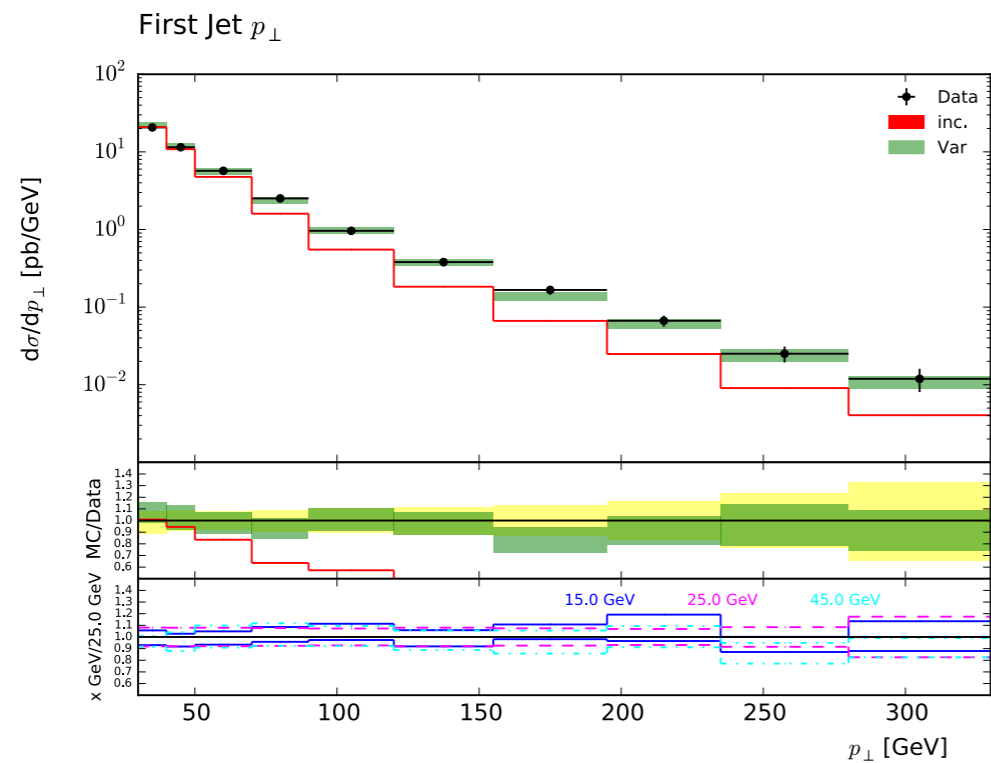
FxFx Z results (2)



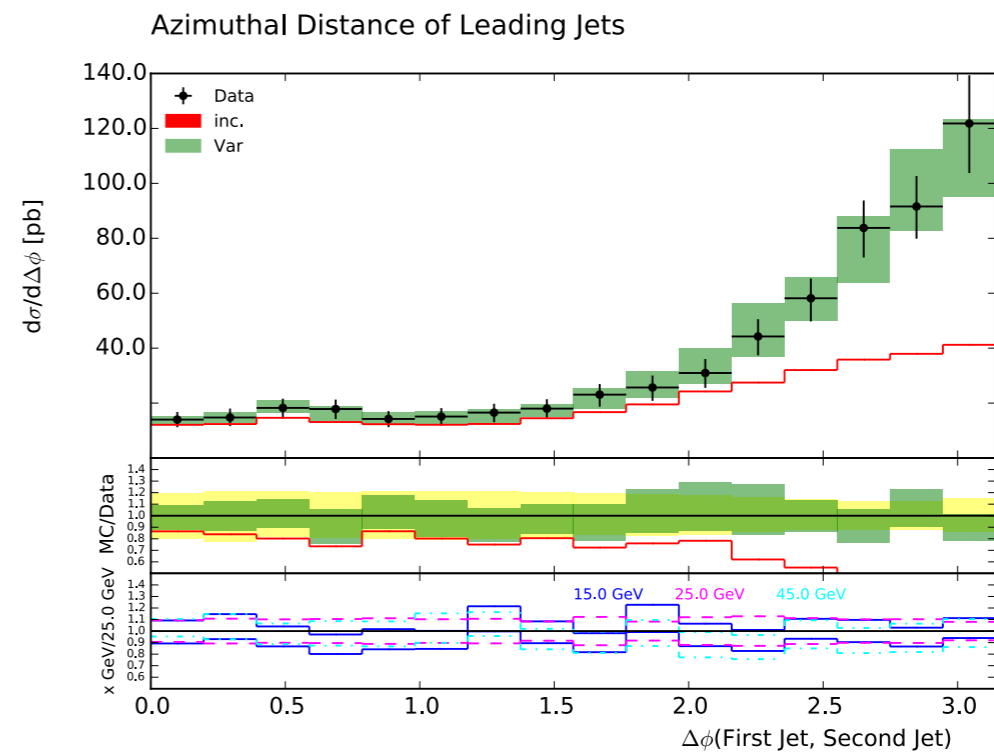
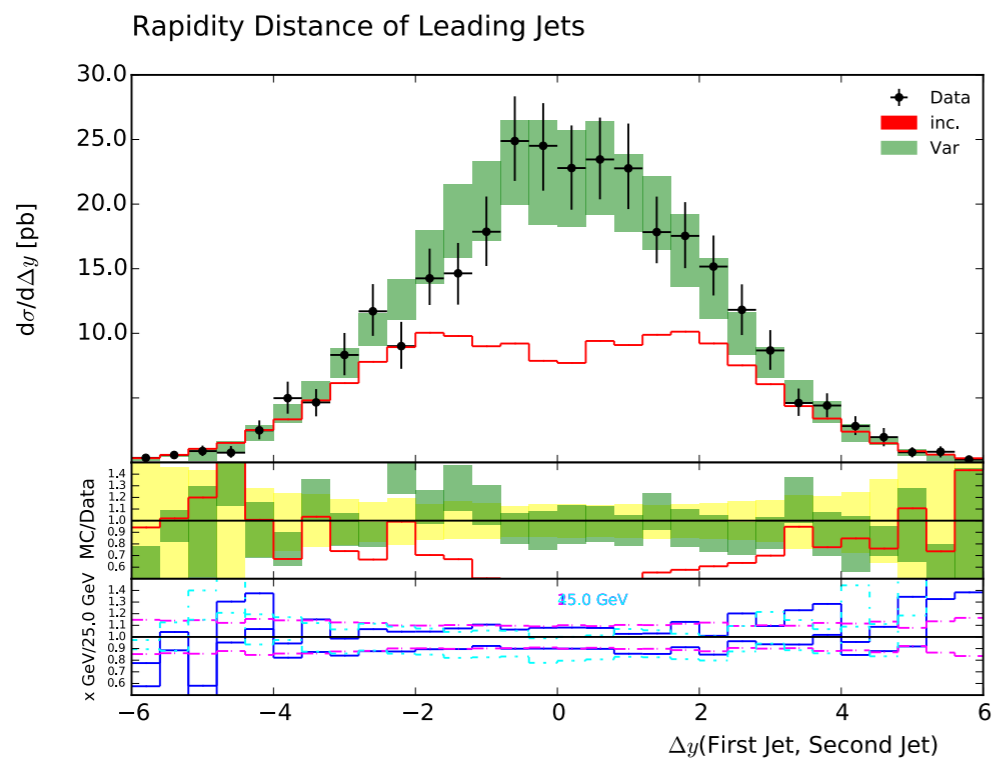
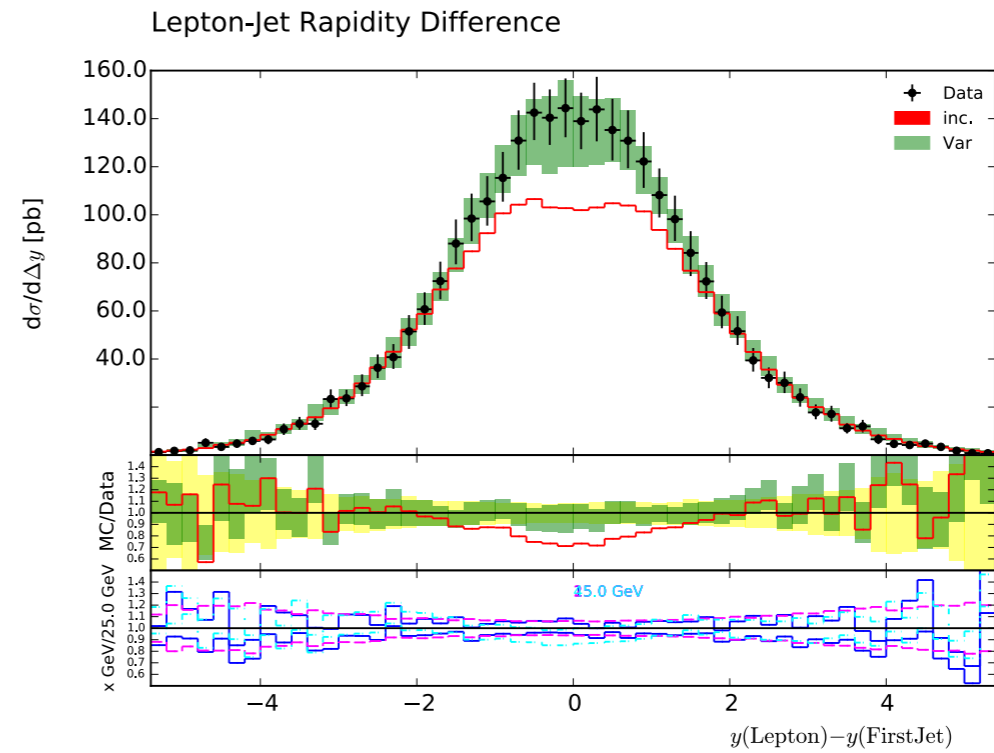
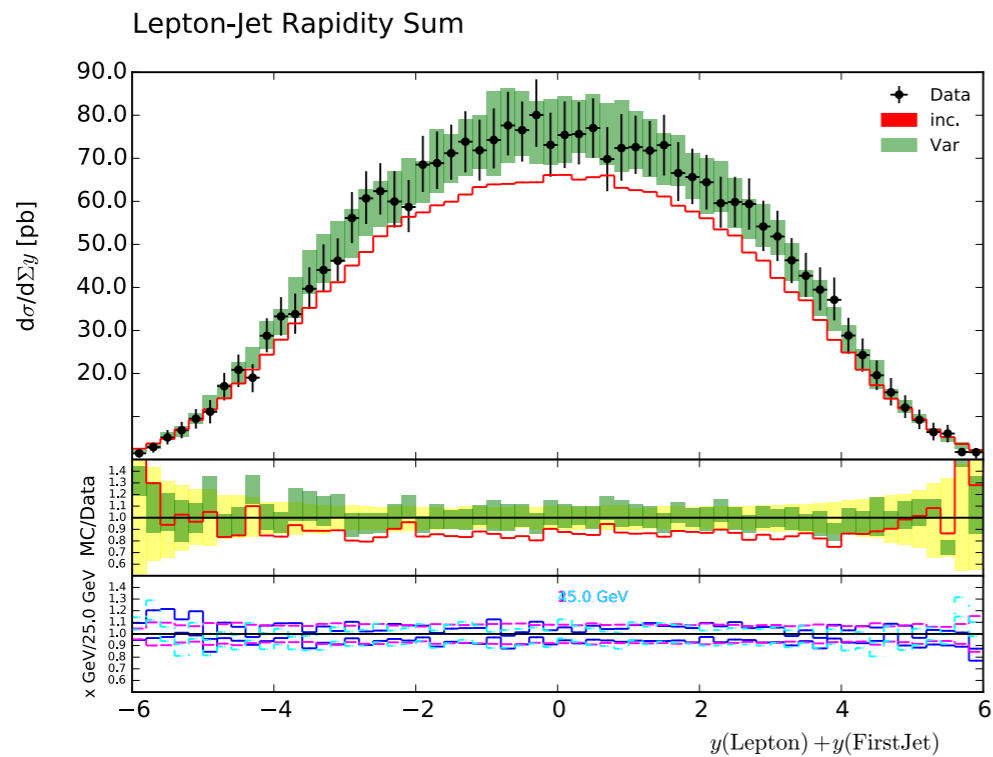
FxFx W results (I)



FxFx W results (2)

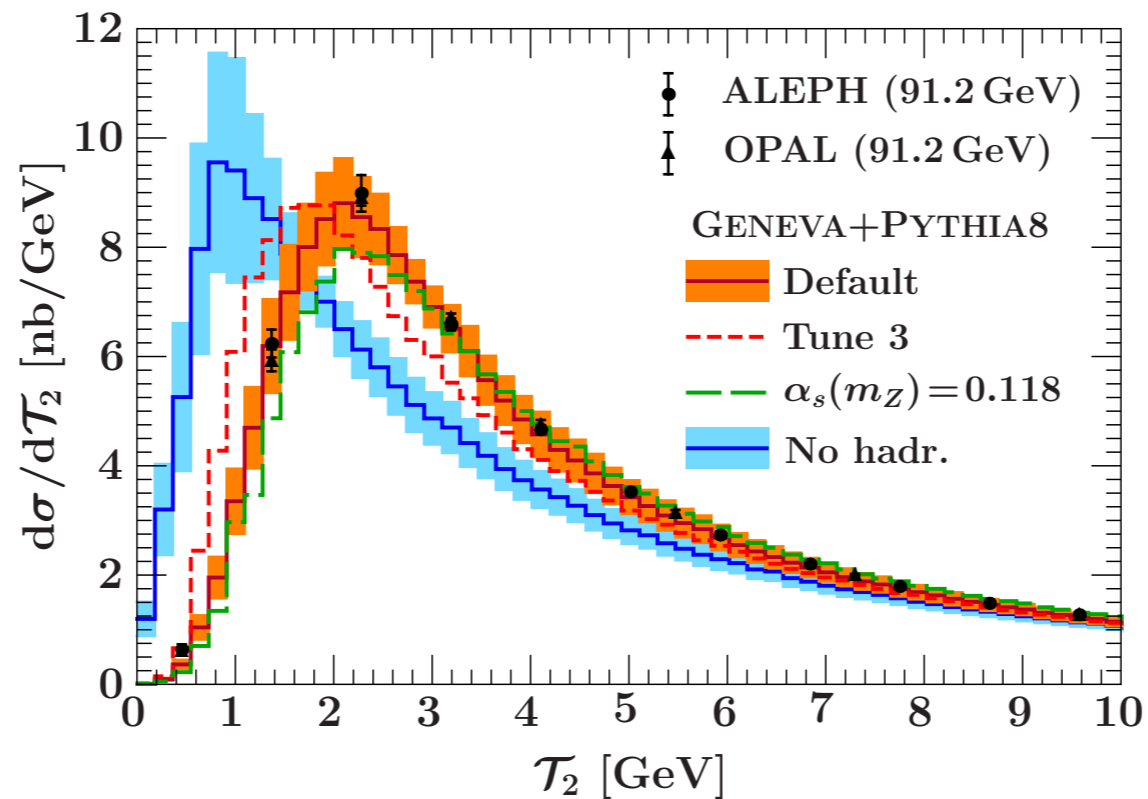
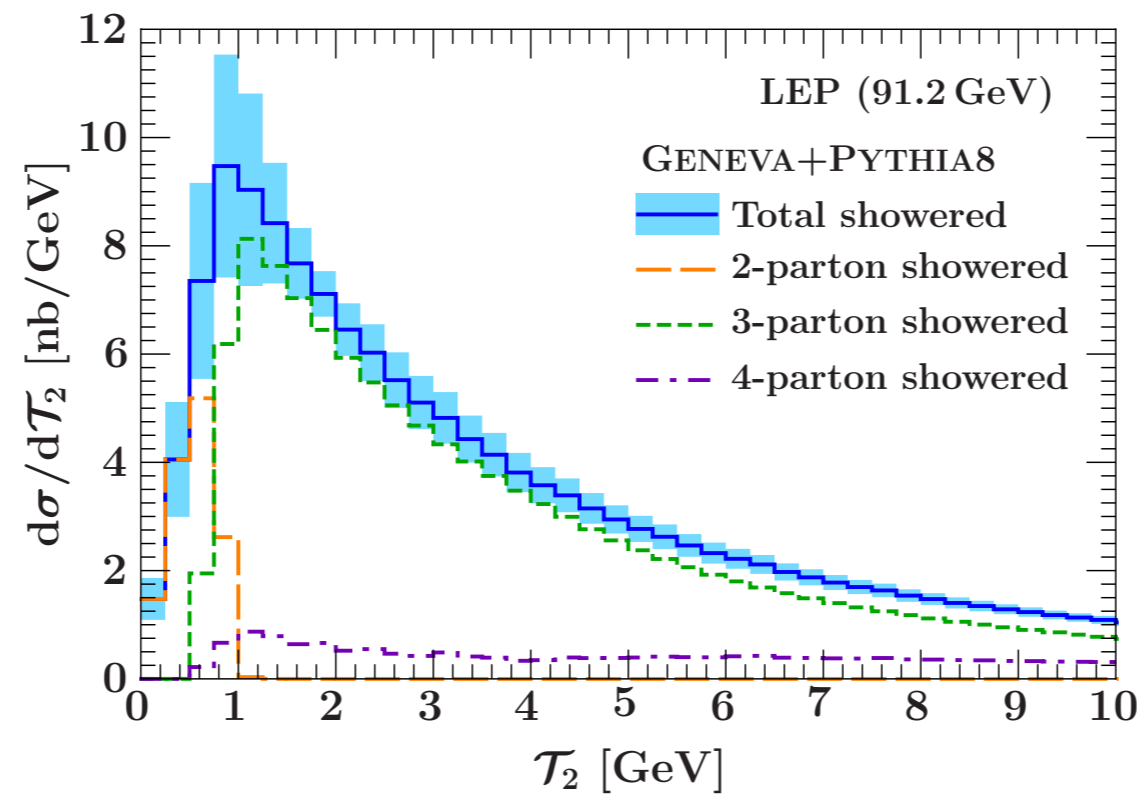


FxFx W results (3)



Geneva merging (e^+e^-)

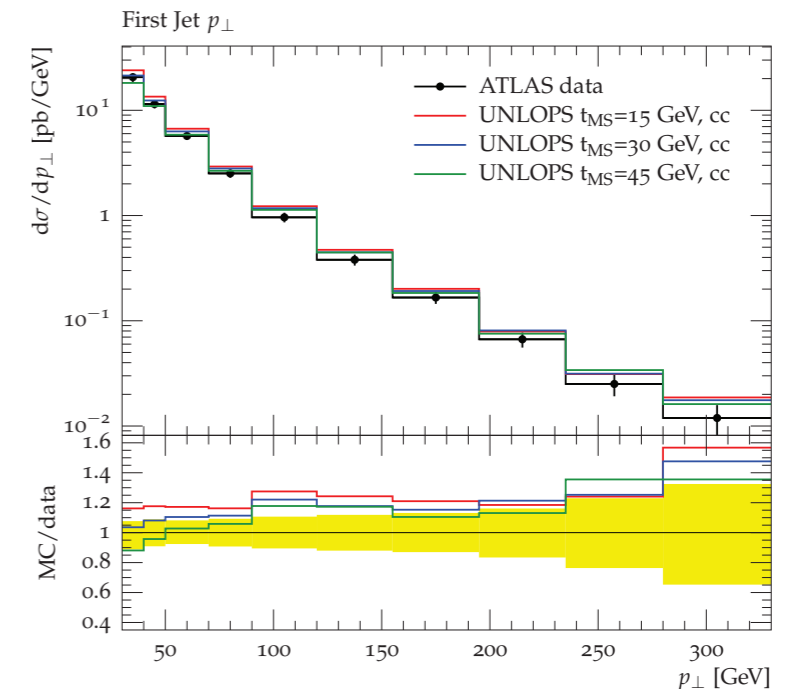
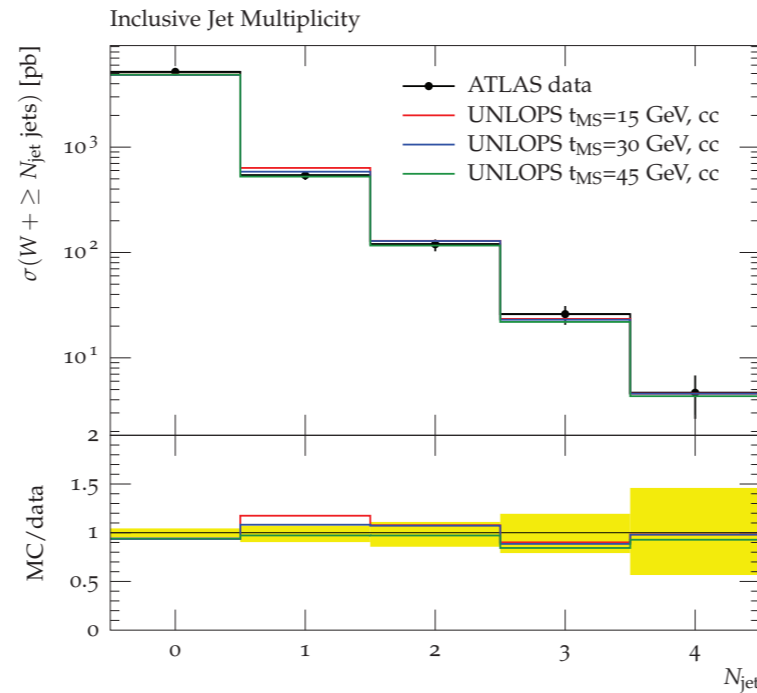
Alioli et al., 1211.7049



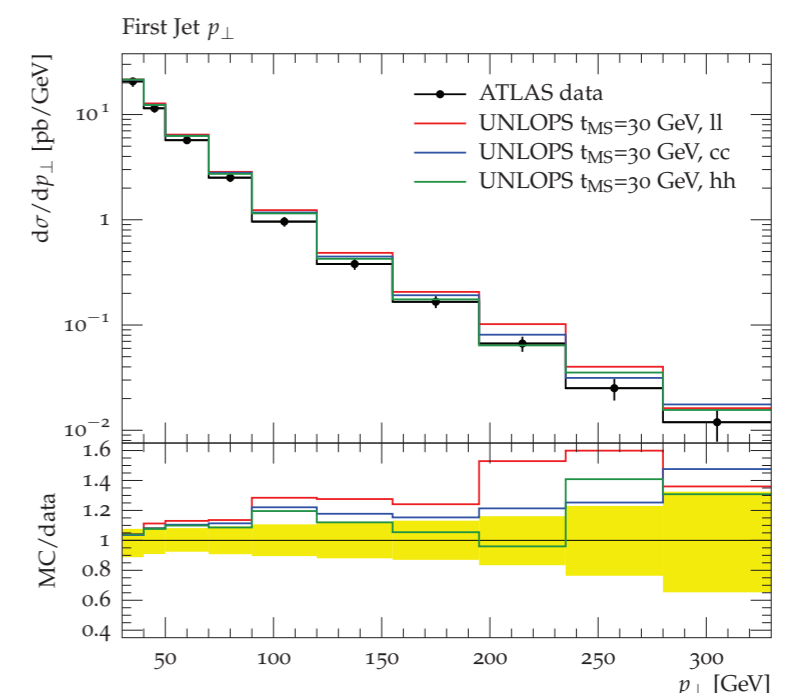
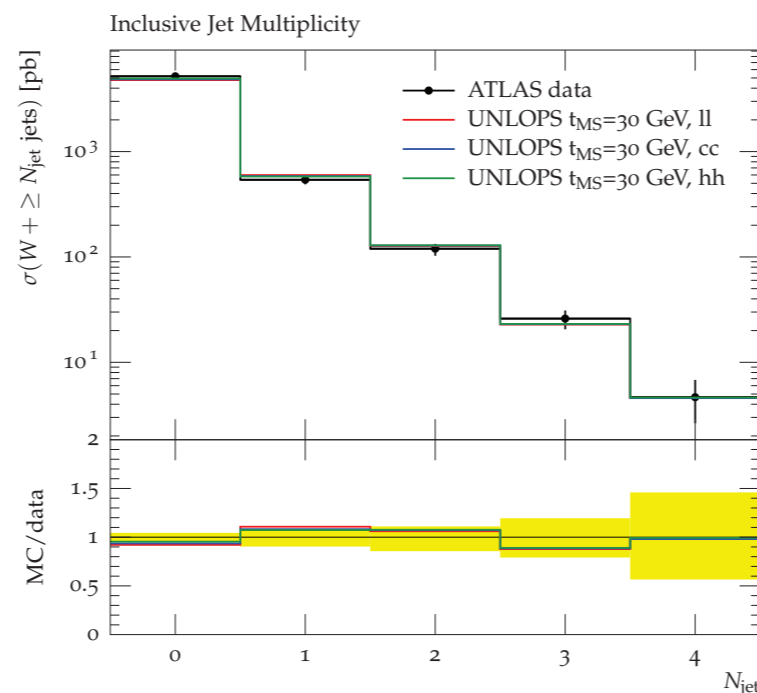
UNLOPS merging

Lönblad, Prestel, 1211.7278

- Merging scale dependence



- Ren/fac scale dependence



Parton Showers

Antenna (Lund) shower

In the rest frame of dipole (jk) , emission i has transverse momentum p_t and rapidity y where

$$p_t^2 = 2 \frac{p_i \cdot p_j p_i \cdot p_k}{p_j \cdot p_k}, \quad (1)$$

$$y = \frac{1}{2} \ln \frac{p_i \cdot p_k}{p_i \cdot p_j} \quad (2)$$

and the leading contribution of this emission is

$$d\sigma_{n+1}^{(jk)} = d\sigma_n \frac{\alpha_s}{2\pi} (-2\mathbf{T}_j \cdot \mathbf{T}_k) \frac{dp_t^2}{p_t^2} dy. \quad (3)$$

The phase space for emission is $p_i \cdot p_j$, $p_i \cdot p_k < p_j \cdot p_k = Q^2/2$ where Q is the dipole mass. Hence

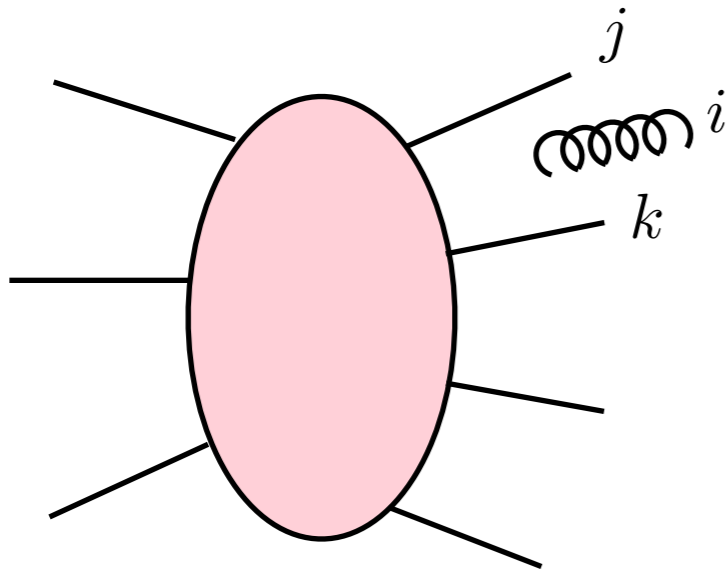
$$-\ln \frac{Q}{p_t} < y < \ln \frac{Q}{p_t}. \quad (4)$$

- **Three jets in e^+e^- annihilation**

The p_t resolution is Q_0 where $Q_0^2/Q^2 = y_{\text{cut}}$. Hence the 3-jet rate is

$$R_3^d = \frac{\alpha_s}{2\pi} 2C_F \int_{Q_0}^Q 2 \frac{dp_t}{p_t} \int_{-\ln Q/p_t}^{\ln Q/p_t} dy = \frac{1}{2} C_F a L^2 \quad (5)$$

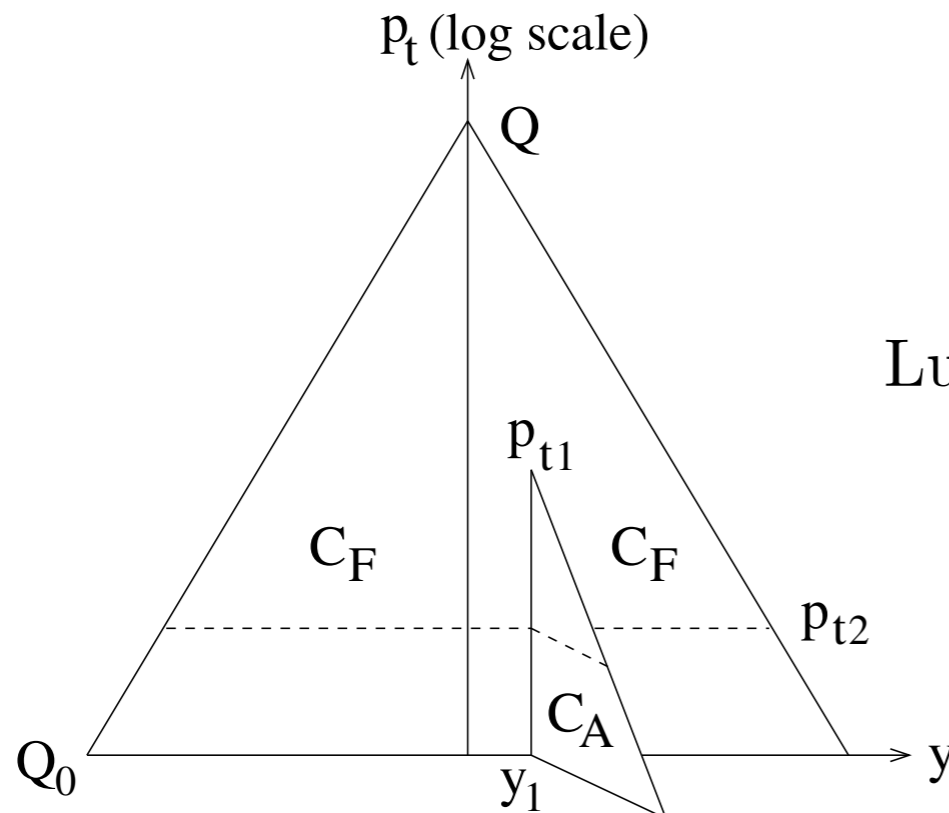
where $a = \alpha_s/\pi$ and $L = \ln y_{\text{cut}}$.



Antenna shower

- Four jets in e^+e^- annihilation

$$\begin{aligned}
 R_4^d &= \left(\frac{\alpha_s}{2\pi}\right)^2 2C_F \int_{Q_0}^Q 2 \frac{dp_{t1}}{p_{t1}} 2 \ln \frac{Q}{p_{t1}} \left[2C_F \int_{Q_0}^{p_{t1}} 2 \frac{dp_{t2}}{p_{t2}} 2 \ln \frac{Q}{p_{t2}} + C_A \int_{Q_0}^{p_{t1}} 2 \frac{dp_{t2}}{p_{t2}} 2 \ln \frac{p_{t1}}{p_{t2}} \right] \\
 &= \left(\frac{\alpha_s}{2\pi}\right)^2 16C_F \int_{Q_0}^Q \frac{dp_{t1}}{p_{t1}} \ln \frac{Q}{p_{t1}} \left[2C_F \left(\ln^2 \frac{Q}{Q_0} - \ln^2 \frac{Q}{p_{t1}} \right) + C_A \ln^2 \frac{p_{t1}}{Q_0} \right] \\
 &= \left(\frac{1}{8} C_F^2 + \frac{1}{48} C_F C_A \right) a^2 L^4,
 \end{aligned}$$



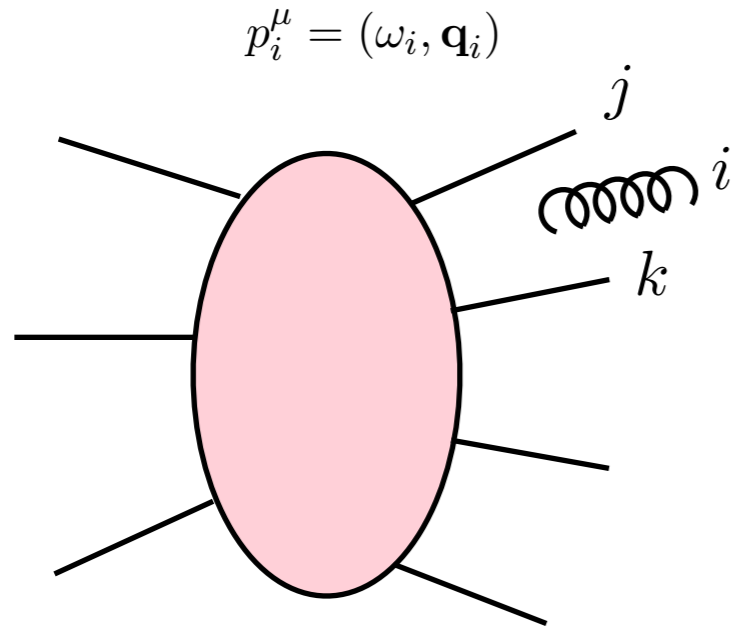
Lund “origami” diagram for $e^+e^- \rightarrow 4$ jets.

Dipole partition

$$D_{jk} = \frac{p_j \cdot p_k}{p_j \cdot q p_k \cdot q} = D_{jk}^{(j)} + D_{jk}^{(k)}$$

- **Catani-Seymour** $D_{jk}^{(j)} = D_{jk} \frac{p_k \cdot q}{(p_j + p_k) \cdot q}$
- **Nagy-Soper** $D_{jk}^{(j)} = D_{jk} \frac{p_k \cdot q p_j \cdot Q}{p_j \cdot q p_k \cdot Q + p_k \cdot q p_j \cdot Q}$
- **Angular-ordered** $D_{jk}^{(j)} = \frac{1}{2} D_{jk} + \frac{1}{2 q \cdot Q} \left(\frac{p_j \cdot Q}{p_j \cdot q} - \frac{p_k \cdot Q}{p_k \cdot q} \right)$

AO parton shower



- Coherent emission from (jk)

$$\begin{aligned} d\sigma_{n+1}^{(jk)} &= g_s^2 d\sigma_n \frac{d^3\mathbf{q}_i}{(2\pi)^3 2\omega_i} (-\mathbf{T}_j \cdot \mathbf{T}_k) \frac{p_j \cdot p_k}{p_j \cdot p_i, p_k \cdot p_i} \\ &= \frac{\alpha_s}{2\pi} d\sigma_n \frac{d\omega_i}{\omega_i} \frac{d\Omega_i}{2\pi} (-\mathbf{T}_j \cdot \mathbf{T}_k) \frac{\xi_{jk}}{\xi_{ij} \xi_{ik}} \end{aligned}$$

where $\xi_{jk} = 1 - \cos \theta_{jk}$. Now

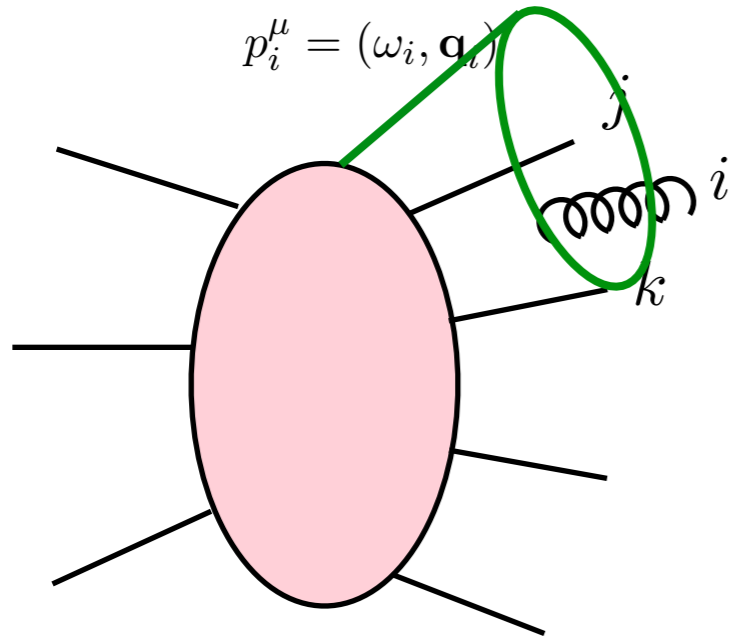
$$\frac{d\Omega_i}{2\pi} \frac{\xi_{jk}}{\xi_{ij} \xi_{ik}} = \frac{d\xi_{ij}}{\xi_{ij}} \frac{d\phi_{ij}}{2\pi} \frac{1}{2} \left(\frac{\xi_{jk} - \xi_{ij}}{\xi_{ik}} + 1 \right) + (j \leftrightarrow k)$$

- After azimuthal integration, this is **exactly**

$$\frac{d\xi_{ij}}{\xi_{ij}} \Theta(\xi_{jk} - \xi_{ij}) + \frac{d\xi_{ik}}{\xi_{ik}} \Theta(\xi_{jk} - \xi_{ik})$$

- Each parton j,k radiates into cone θ_{ij} , $\theta_{ik} < \theta_{jk}$

AO parton shower



- Coherent emission from (jk)

$$\begin{aligned}
 d\sigma_{n+1}^{(jk)} &= g_s^2 d\sigma_n \frac{d^3\mathbf{q}_i}{(2\pi)^3 2\omega_i} (-\mathbf{T}_j \cdot \mathbf{T}_k) \frac{p_j \cdot p_k}{p_j \cdot p_i, p_k \cdot p_i} \\
 &= \frac{\alpha_s}{2\pi} d\sigma_n \frac{d\omega_i}{\omega_i} \frac{d\Omega_i}{2\pi} (-\mathbf{T}_j \cdot \mathbf{T}_k) \frac{\xi_{jk}}{\xi_{ij} \xi_{ik}}
 \end{aligned}$$

where $\xi_{jk} = 1 - \cos \theta_{jk}$. Now

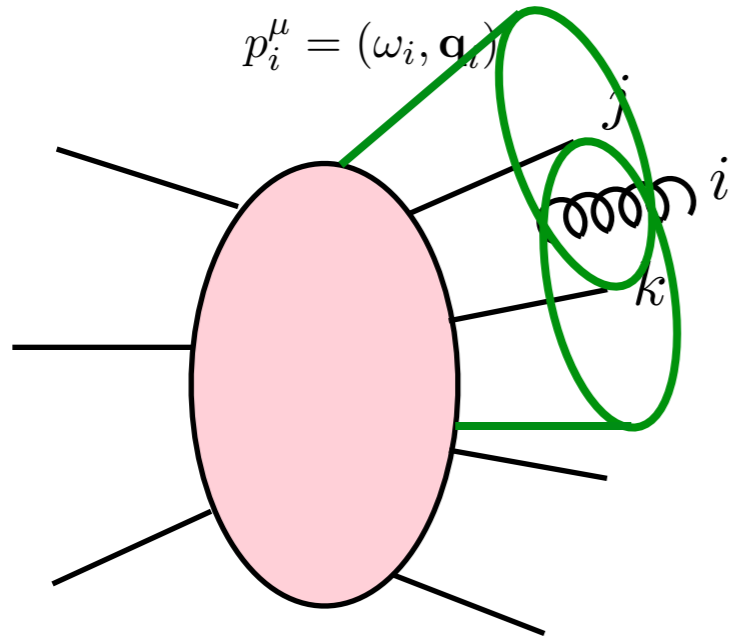
$$\frac{d\Omega_i}{2\pi} \frac{\xi_{jk}}{\xi_{ij} \xi_{ik}} = \frac{d\xi_{ij}}{\xi_{ij}} \frac{d\phi_{ij}}{2\pi} \frac{1}{2} \left(\frac{\xi_{jk} - \xi_{ij}}{\xi_{ik}} + 1 \right) + (j \leftrightarrow k)$$

- After azimuthal integration, this is **exactly**

$$\frac{d\xi_{ij}}{\xi_{ij}} \Theta(\xi_{jk} - \xi_{ij}) + \frac{d\xi_{ik}}{\xi_{ik}} \Theta(\xi_{jk} - \xi_{ik})$$

- Each parton j,k radiates into cone θ_{ij} , $\theta_{ik} < \theta_{jk}$

AO parton shower



- Coherent emission from (jk)

$$\begin{aligned} d\sigma_{n+1}^{(jk)} &= g_s^2 d\sigma_n \frac{d^3\mathbf{q}_i}{(2\pi)^3 2\omega_i} (-\mathbf{T}_j \cdot \mathbf{T}_k) \frac{p_j \cdot p_k}{p_j \cdot p_i, p_k \cdot p_i} \\ &= \frac{\alpha_s}{2\pi} d\sigma_n \frac{d\omega_i}{\omega_i} \frac{d\Omega_i}{2\pi} (-\mathbf{T}_j \cdot \mathbf{T}_k) \frac{\xi_{jk}}{\xi_{ij} \xi_{ik}} \end{aligned}$$

where $\xi_{jk} = 1 - \cos \theta_{jk}$. Now

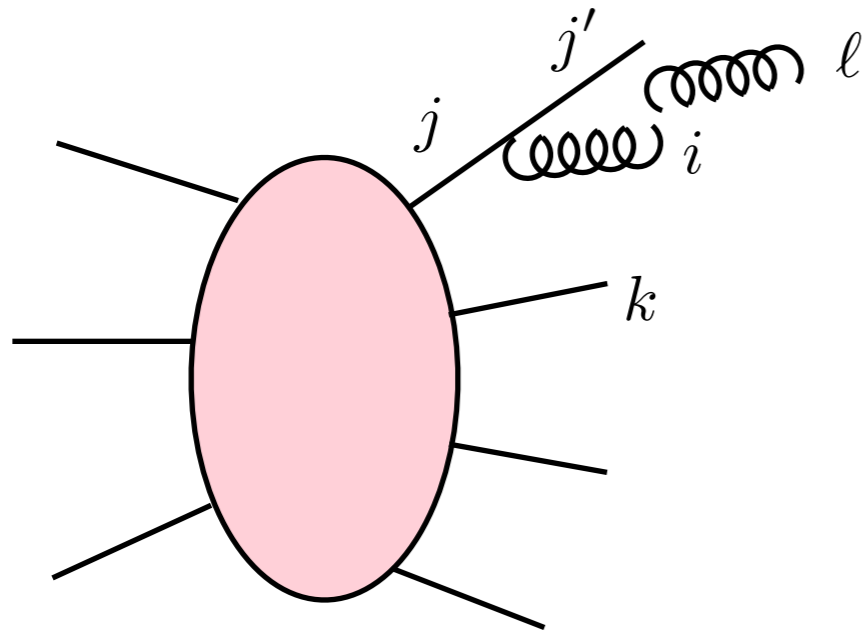
$$\frac{d\Omega_i}{2\pi} \frac{\xi_{jk}}{\xi_{ij} \xi_{ik}} = \frac{d\xi_{ij}}{\xi_{ij}} \frac{d\phi_{ij}}{2\pi} \frac{1}{2} \left(\frac{\xi_{jk} - \xi_{ij}}{\xi_{ik}} + 1 \right) + (j \leftrightarrow k)$$

- After azimuthal integration, this is **exactly**

$$\frac{d\xi_{ij}}{\xi_{ij}} \Theta(\xi_{jk} - \xi_{ij}) + \frac{d\xi_{ik}}{\xi_{ik}} \Theta(\xi_{jk} - \xi_{ik})$$

- Each parton j radiates into cone $\theta_{ij} < \theta_{jk}$

AO parton shower



- Two gluon emission

$$d\sigma_{n+2}^{(ij)} = \frac{\alpha_s}{\pi} d\sigma_{n+1}^{(j)} \frac{d\omega_\ell}{\omega_\ell} \left\{ (-\mathbf{T}_i \cdot \mathbf{T}'_j) \int^{\xi_{ij}} \left(\frac{d\xi_{li}}{\xi_{li}} + \frac{d\xi_{lj}}{\xi_{lj}} \right) + \sum_{k \neq i,j} \left[(-\mathbf{T}_i \cdot \mathbf{T}_k) \int^{\xi_{ik}} \frac{d\xi_{li}}{\xi_{li}} + (-\mathbf{T}'_j \cdot \mathbf{T}_k) \int^{\xi_{jk}} \frac{d\xi_{lj}}{\xi_{lj}} \right] \right\}$$

where $\mathbf{T}'_j = \mathbf{T}_j - \mathbf{T}_i$ and $\mathbf{T}_i + \mathbf{T}'_j + \sum_{k \neq i,j} \mathbf{T}_k = 0$

- Collecting terms in ξ_{li} and ξ_{lj} , we find

$$d\sigma_{n+2}^{(ij)} = \frac{\alpha_s}{\pi} d\sigma_{n+1}^{(j)} \frac{d\omega_\ell}{\omega_\ell} \left\{ \mathbf{T}_i \cdot \mathbf{T}_i \int^{\xi_{ij}} \frac{d\xi_{li}}{\xi_{li}} + \mathbf{T}'_j \cdot \mathbf{T}'_j \int^{\xi_{ij}} \frac{d\xi_{lj}}{\xi_{lj}} \right. \left. - \mathbf{T}_j \cdot \sum_{k \neq i,j} \mathbf{T}_k \int_{\xi_{ij}}^{\xi_{jk}} \frac{d\xi_{lj}}{\xi_{lj}} \right. \left. - \mathbf{T}_i \cdot \sum_{k \neq i,j} \mathbf{T}_k \left(\int_{\xi_{ij}}^{\xi_{ik}} \frac{d\xi_{li}}{\xi_{li}} - \int_{\xi_{ij}}^{\xi_{jk}} \frac{d\xi_{lj}}{\xi_{lj}} \right) \right\}$$

Annotations:

- each parton emits into its cone (points to $\mathbf{T}'_j \cdot \mathbf{T}'_j \int^{\xi_{ij}} \frac{d\xi_{lj}}{\xi_{lj}}$)
- coherent emission outside cones, done in previous step (points to $-\mathbf{T}_j \cdot \sum_{k \neq i,j} \mathbf{T}_k \int_{\xi_{ij}}^{\xi_{jk}} \frac{d\xi_{lj}}{\xi_{lj}}$)
- non-singular, 2 logs down, neglected (points to $-\mathbf{T}_i \cdot \sum_{k \neq i,j} \mathbf{T}_k \left(\int_{\xi_{ij}}^{\xi_{ik}} \frac{d\xi_{li}}{\xi_{li}} - \int_{\xi_{ij}}^{\xi_{jk}} \frac{d\xi_{lj}}{\xi_{lj}} \right)$)

$e^+e^- \rightarrow q\bar{q}gg$

- AO parton shower:

$$d\sigma_{n+2}^{(ij)} = \frac{\alpha_S}{\pi} d\sigma_{n+1}^{(j)} \frac{d\omega_\ell}{\omega_\ell} \left\{ \mathbf{T}_i \cdot \mathbf{T}_i \int^{\xi_{ij}} \frac{d\xi_{li}}{\xi_{li}} + \mathbf{T}'_j \cdot \mathbf{T}'_j \int^{\xi_{ij}} \frac{d\xi_{lj}}{\xi_{lj}} - \mathbf{T}_j \cdot \sum_{k \neq i,j} \mathbf{T}_k \int_{\xi_{ij}}^{\xi_{jk}} \frac{d\xi_{lj}}{\xi_{lj}} \right\}$$

→ $d\sigma_4^{(iq)} = \frac{\alpha_S}{\pi} d\sigma_3^{(q)} \frac{d\omega_\ell}{\omega_\ell} \left\{ C_A \int^{\xi_{iq}} \frac{d\xi_{li}}{\xi_{li}} + C_F \int^{\xi_{q\bar{q}}} \frac{d\xi_{lq}}{\xi_{lq}} \right\}$ where $d\sigma_3^{(q)} = \frac{\alpha_S}{\pi} \sigma_2 C_F \frac{d\omega_i}{\omega_i} \int^{\xi_{q\bar{q}}} \frac{d\xi_{iq}}{\xi_{iq}}$

- 4-jet rate (k_t -algorithm):

$$y_{lq} = 2\omega_\ell^2 \xi_{lq} / Q^2 > y_c, \quad y_{li} = 2\omega_m^2 \xi_{li} / Q^2 > y_c \quad \text{where } \omega_m = \min\{\omega_\ell, \omega_i\}$$

$$\sigma_4^{(iq)} = \left(\frac{\alpha_S}{\pi} \right)^2 \sigma_2 C_F \int_{Q\sqrt{y_c}/2}^{Q/2} \frac{d\omega_i}{\omega_i} \int_{Q\sqrt{y_c}/2}^{Q/2} \frac{d\omega_\ell}{\omega_\ell} \int_{Q^2 y_c / 2\omega_i^2}^2 \frac{d\xi_{iq}}{\xi_{iq}} \left\{ C_A \ln \left(\frac{2\omega_m^2 \xi_{iq}}{Q^2 y_c} \right) + C_F \ln \left(\frac{4\omega_\ell^2}{Q^2 y_c} \right) \right\}$$

→ $R_4 = (\sigma_4^{(iq)} + \sigma_4^{(i\bar{q})}) / \sigma_2 = \left(\frac{\alpha_S}{\pi} \right)^2 C_F \left(\frac{1}{8} C_F + \frac{1}{48} C_A \right) L^4$ where $L = \log(1/y_c)$

$e^+e^- \rightarrow q\bar{q}ggg$

- 4-jet rate (k_t -algorithm) vs $L = \log(1/y_{\text{cut}})$

$$\frac{1}{\sigma_B} \frac{d\sigma_4}{dL} = \left[\frac{\alpha_S(s)}{\pi} \right]^2 (4AL^3 + 3BL^2 + 2CL + \dots)$$

$$A = C_F^2/8 + C_F C_A/48$$

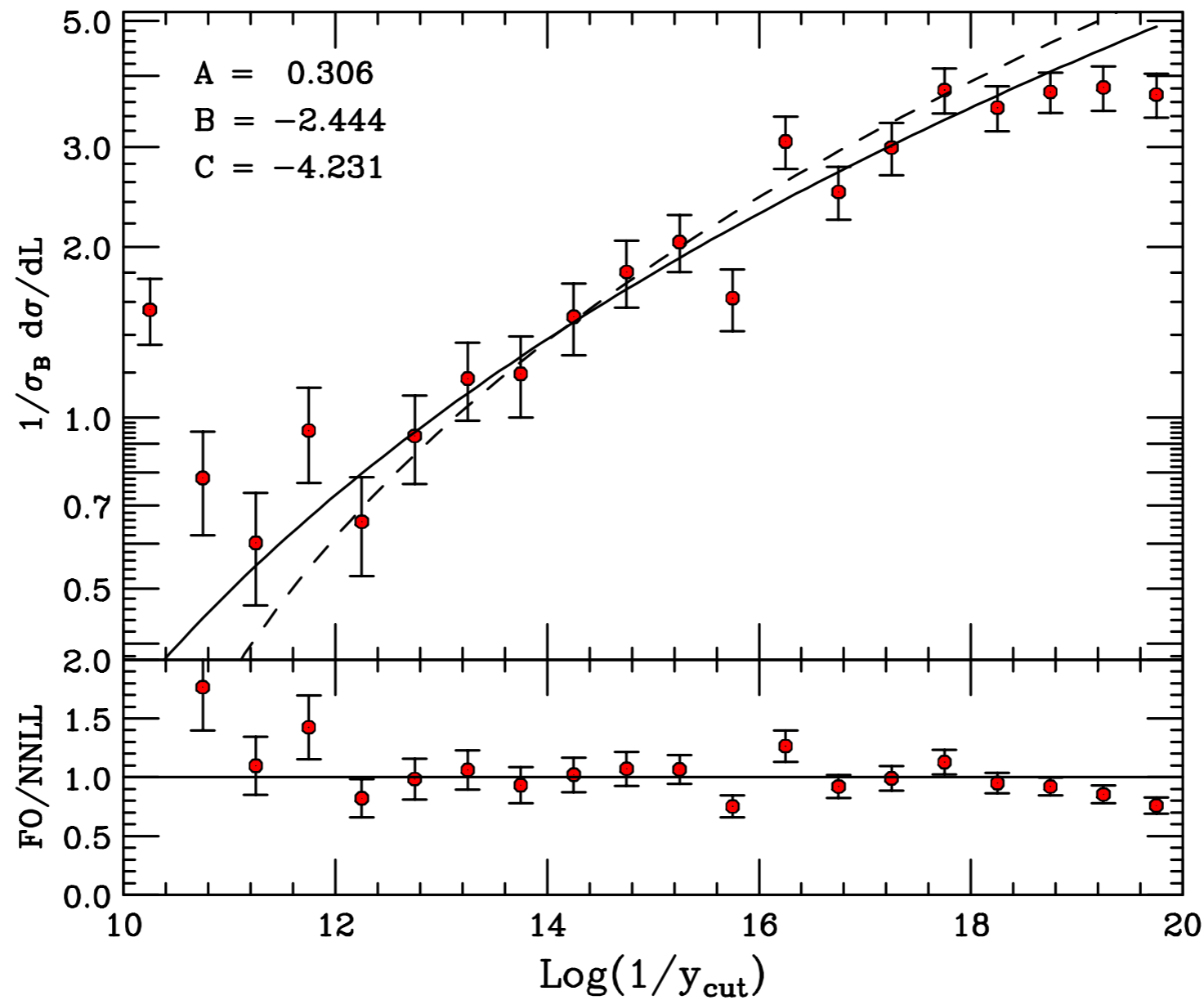
$$B = -3C_F^2/4 - 5C_F C_A/18$$

$$C = ?? \text{ (fitted)}$$

- Compare with MadGraph5 at 1 TeV

✿ $M_{ij} > 100 \text{ MeV} \rightarrow L < 18.4$

$e^+e^- \rightarrow q\bar{q}ggg$



- Dashed is LCA (refitting C)

$e^+e^- \rightarrow q\bar{q}gggg$

- 5-jet rate (k_t -algorithm) vs $L = \log(1/y_{\text{cut}})$

$$\frac{1}{\sigma_B} \frac{d\sigma_5}{dL} = \left[\frac{\alpha_S(s)}{\pi} \right]^3 (6AL^5 + 5BL^4 + 4CL^3 + \dots)$$

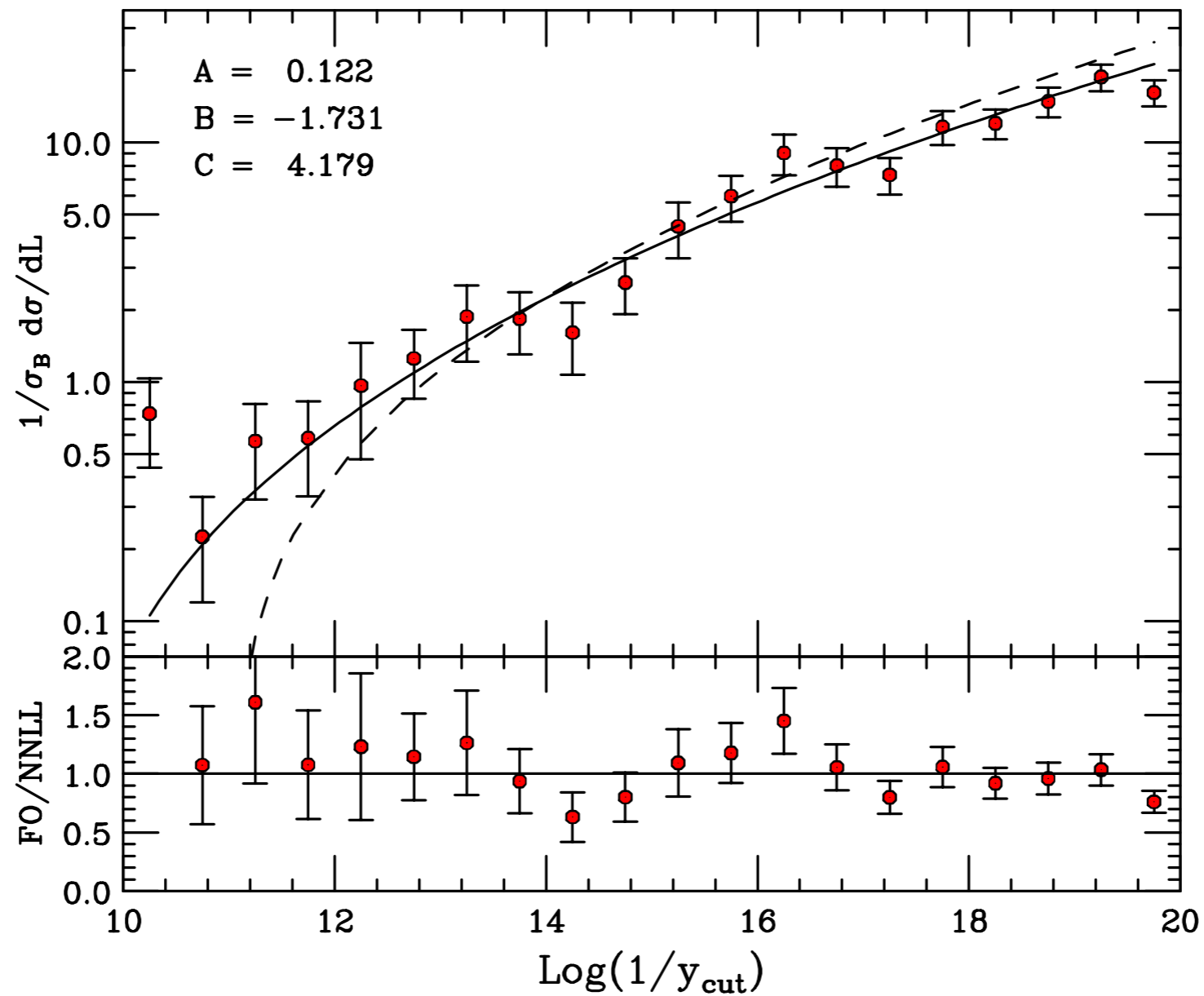
$$A = C_F^3/48 + C_F^2 C_A/96 + C_F C_A^2/720$$

$$B = -3C_F^3/16 - 49C_F^2 C_A/288 - 91C_F C_A^2/2880$$

$$C = ?? \text{ (fitted)}$$

- Compare with MadGraph5 at 1 TeV again

$$e^+ e^- \rightarrow q \bar{q} g g g$$



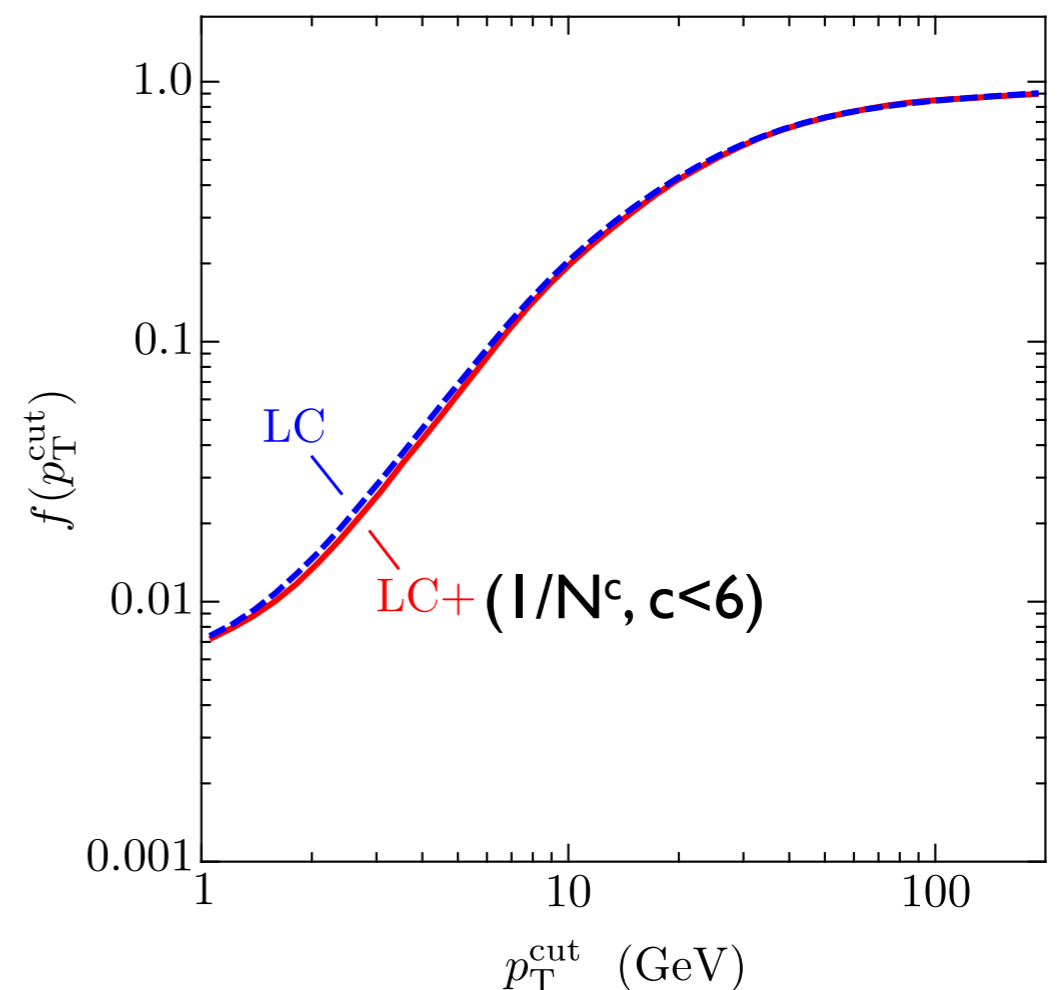
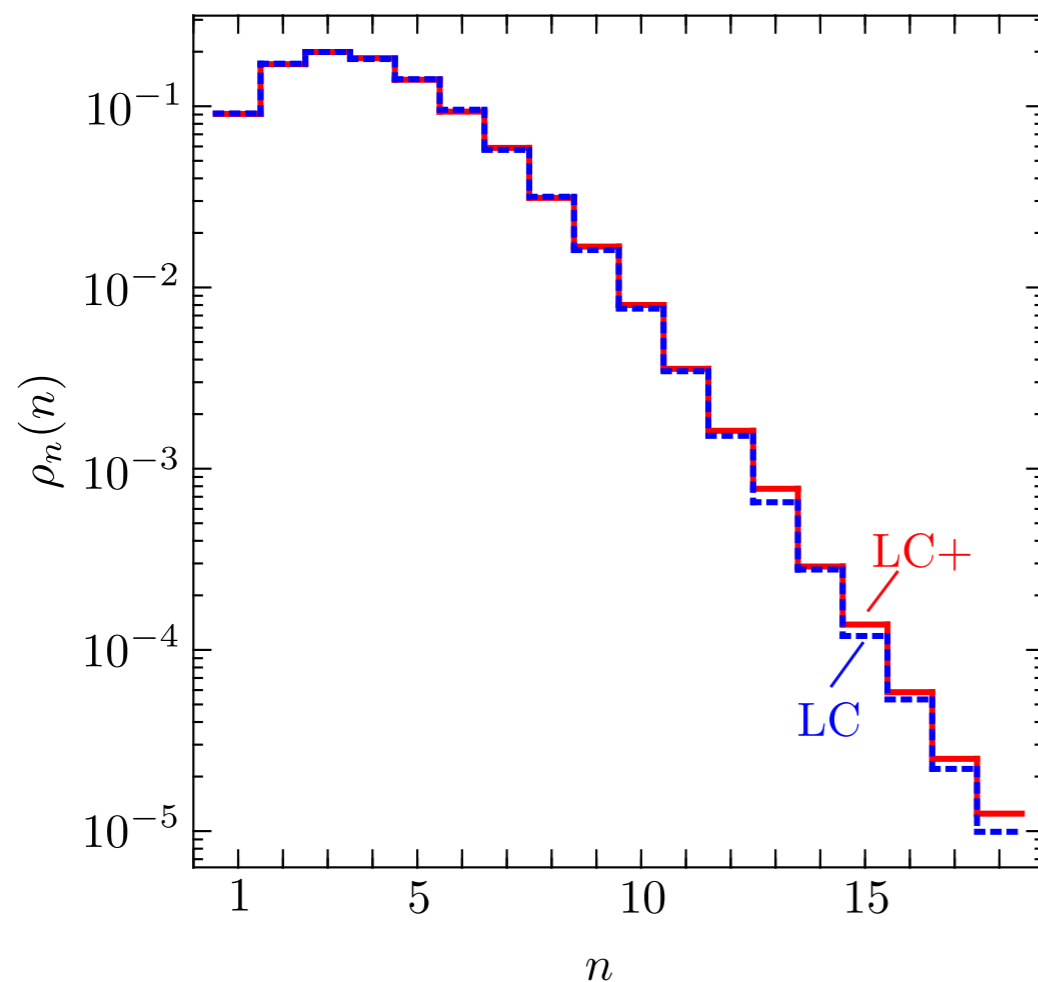
- Dashed is LCA (refitting C)

Subleading colour

- DEDUCTOR pp at 14 TeV
- Number of partons
($p_{T\text{jet}} > 200 \text{ GeV}$, $k_{t\text{min}} = 1 \text{ GeV}$)

Nagy, Soper, 1202.4496, 1501.00778

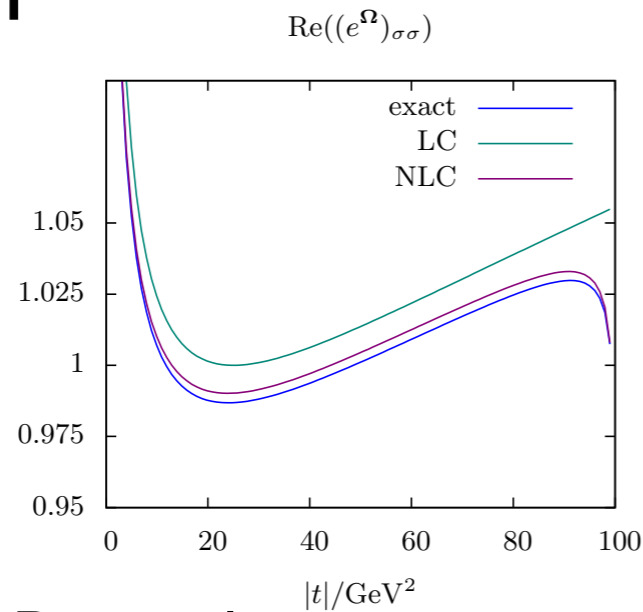
- Gap fraction ($|y| < 2$)



Subleading colour

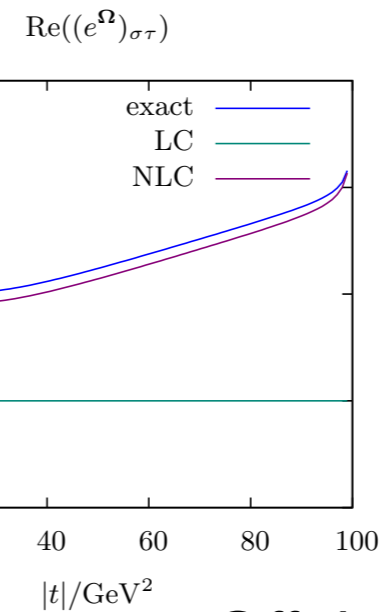
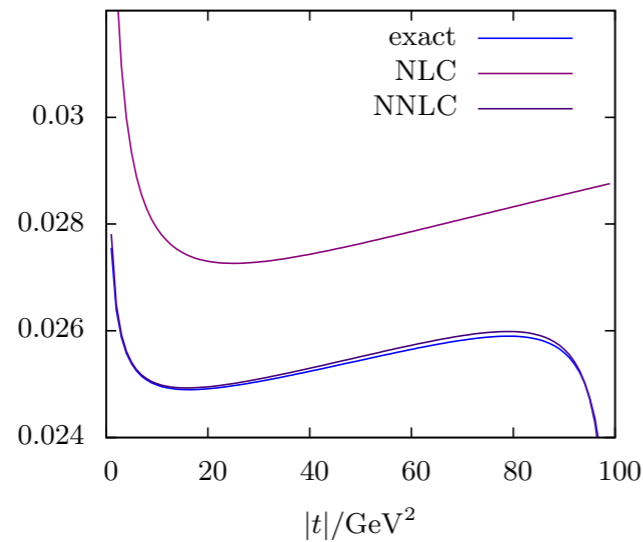
- $q q \rightarrow q q$ evolution matrix elements

Plätzer, I 3 | 2.2448



Diagonal

$\text{Im}((e^\Omega)_{\sigma\sigma})$



Off-diagonal

$\text{Im}((e^\Omega)_{\sigma\tau})$

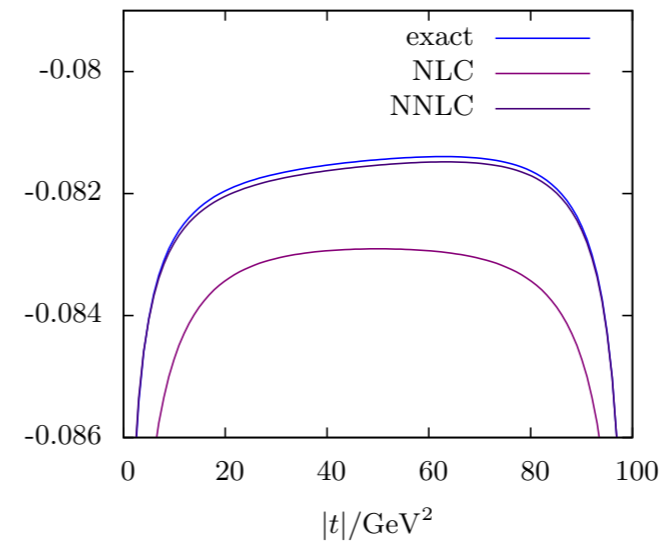
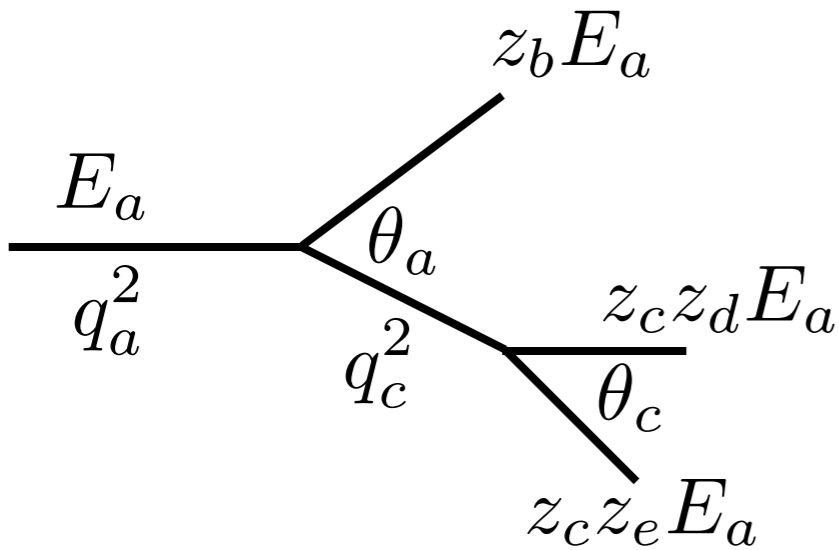


Fig. 3. Real and imaginary parts of a diagonal evolution matrix element for quark-quark scattering at $s = 100 \text{ GeV}^2$, $\mu^2 = 25 \text{ GeV}^2$ as a function of the momentum transfer $|t|$, comparing the exact results to various approximations. This matrix elements describes the amplitude to keep a t -channel colour flow σ .

Fig. 4. Same as figure 3 for an off-diagonal matrix element. The matrix element considered describes the transition from a u -channel colour flow τ to a t -channel one, σ .

Shower ordering

- **Virtuality-ordered shower**

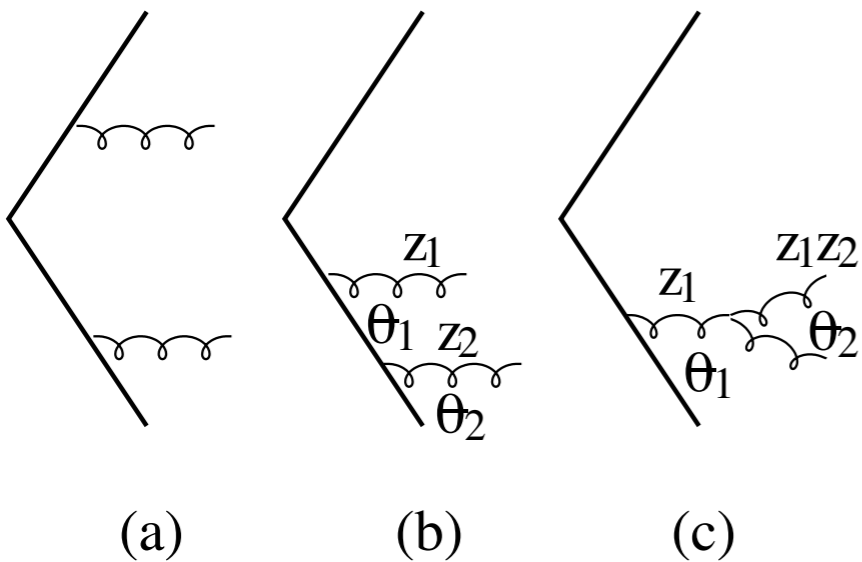


$$q_a^2 = \frac{q_b^2}{z_b} + \frac{q_c^2}{z_c} + \frac{q_T^2}{z_b z_c}$$

$$q_T \simeq z_b z_c E_a \theta_a \quad q_a^2 \simeq z_b z_c (E_a \theta_a)^2$$

$$q_c^2 \simeq z_c^2 z_d z_e (E_a \theta_c)^2 < z_c q_a^2 \simeq z_c^2 z_b (E_a \theta_a)^2$$

$$z_d z_e \theta_c^2 < z_b \theta_a^2$$



- (b) $z_2 \theta_2^2 < z_1 \theta_1^2$ → same as AO
- (c) $z_2 \theta_2^2 < \theta_1^2$ → larger than AO

$$\rightarrow R_4^{q^2} = \left(\frac{\alpha_S}{\pi}\right)^2 \frac{C_F}{8} \left(C_F + \frac{1}{4} C_A\right) L^4$$

← $\frac{25}{12}$

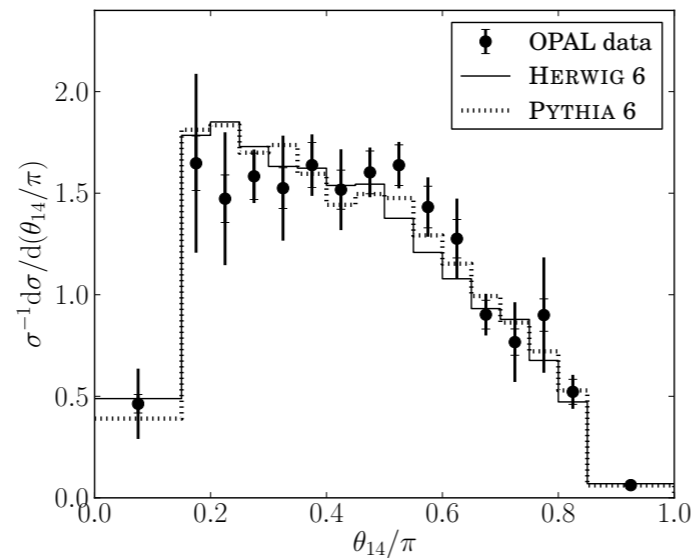
$$\text{vs } R_4^{\text{AO}} = \left(\frac{\alpha_S}{\pi}\right)^2 \frac{C_F}{8} \left(C_F + \frac{1}{6} C_A\right) L^4$$

← $\frac{22}{12}$

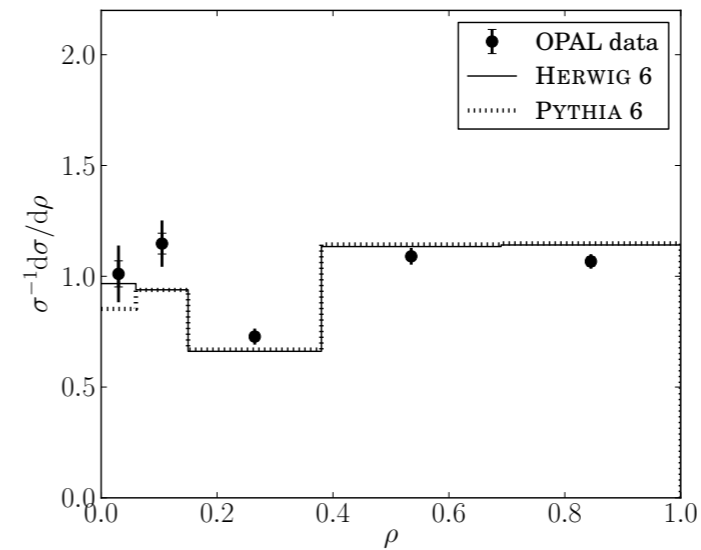
Coherence tests

- $Z^0 \rightarrow 4$ jets (LEP OPAL data) Fischer et al., I505.01636

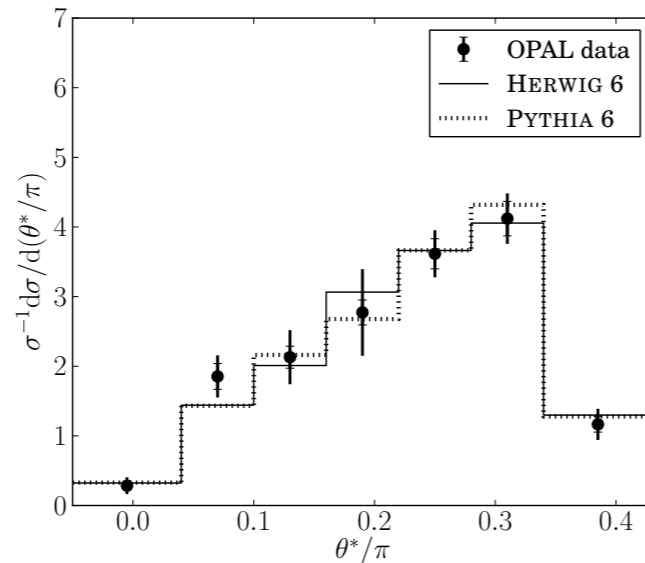
a) Angle between 1st and 4th jet, θ_{14}/π



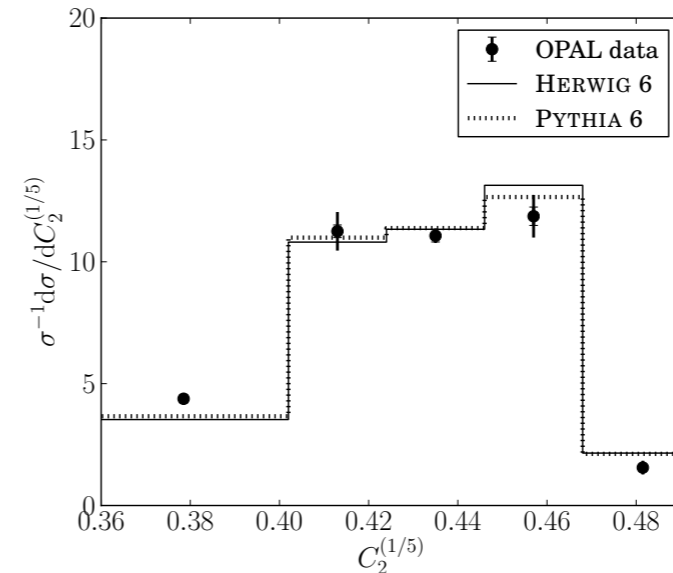
b) Ratio of jet masses, ρ



c) Difference in opening angles, $\theta^* = \theta_{24} - \theta_{23}$



d) 2-point double ratio, $C_2^{(1/5)}$

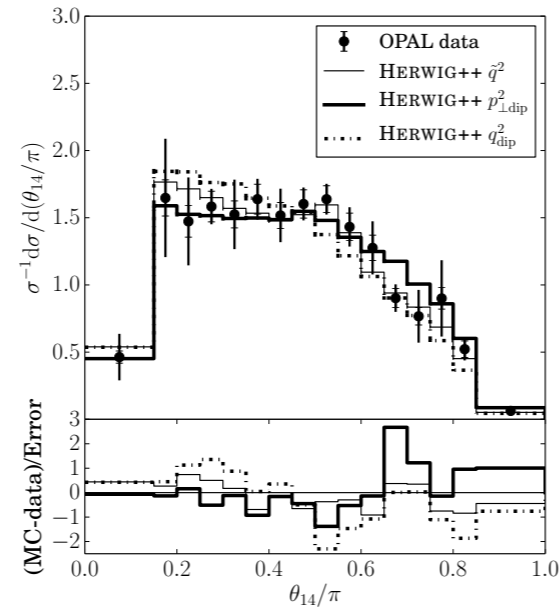


- Herwig 6, Pythia 6 comparisons

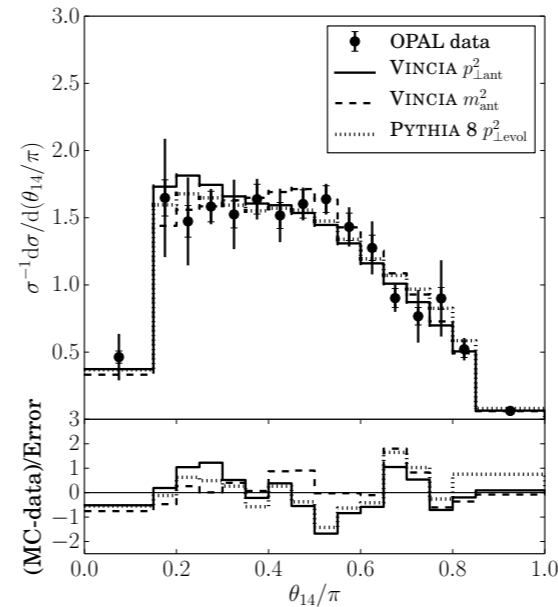
Coherence tests

- $Z^0 \rightarrow 4$ jets (LEP OPAL data) Fischer et al., I505.01636

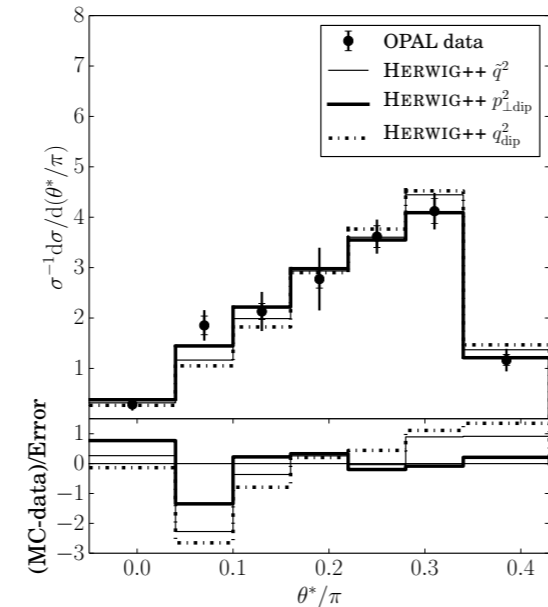
a) Angle between 1st and 4th jet, θ_{14} , HERWIG++



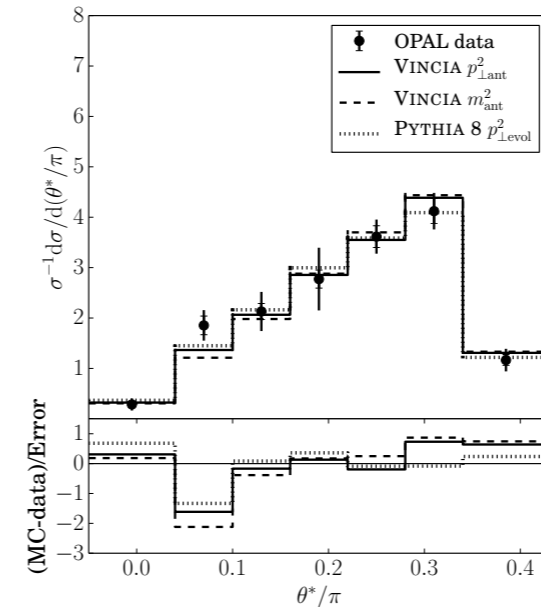
b) Angle between 1st and 4th jet, θ_{14} , VINCIA, PYTHIA 8



a) Difference in opening angles, θ^* , HERWIG++



b) Difference in opening angles, θ^* , VINCIA, PYTHIA 8

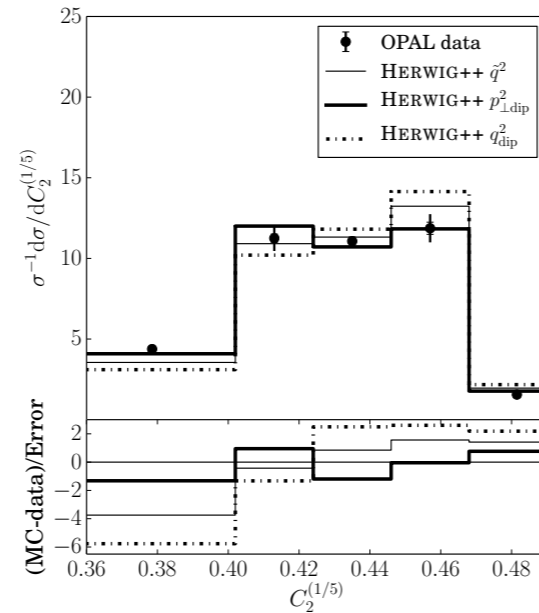


- Herwig++, Pythia 8 comparisons

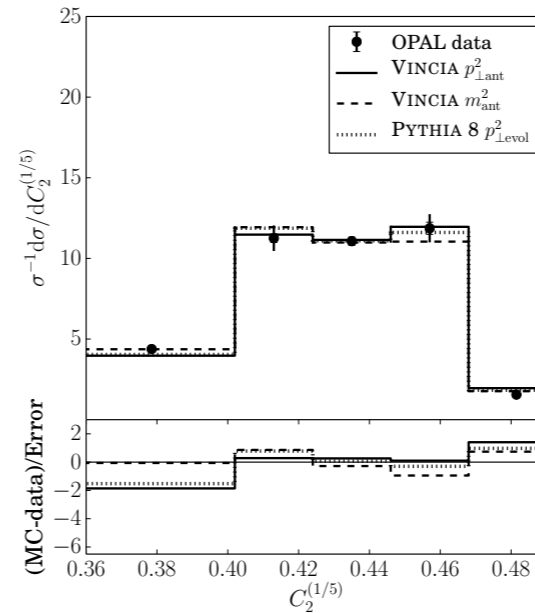
Coherence tests

- $Z^0 \rightarrow 4$ jets (LEP OPAL data) Fischer et al., I505.01636

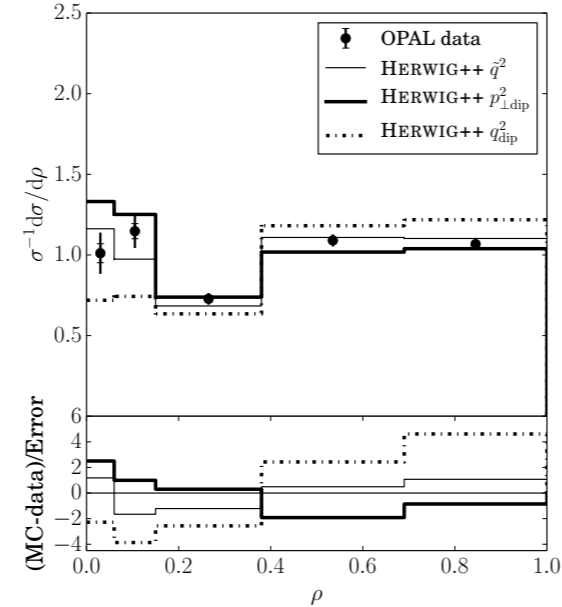
a) 2-point double ratio, $C_2^{(1/5)}$, HERWIG++



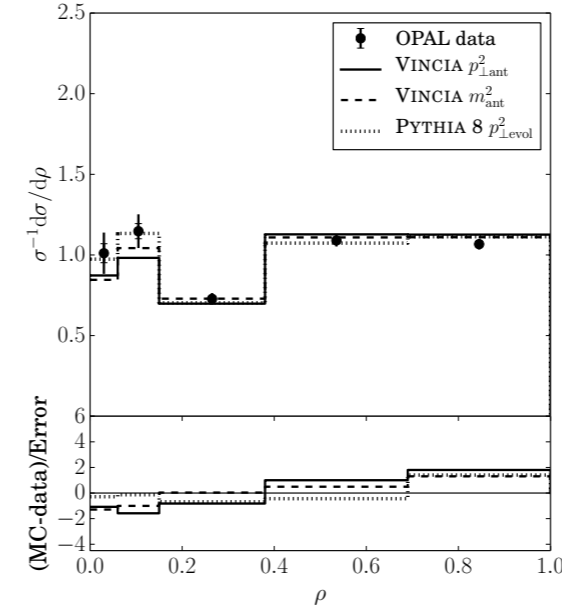
b) 2-point double ratio, $C_2^{(1/5)}$, VINCIA, PYTHIA 8



a) Ratio of jet masses, ρ , HERWIG++



b) Ratio of jet masses, ρ , VINCIA, PYTHIA 8



- Herwig++ virtuality ordering does worst

Spin in showers

$$\langle s | \hat{P}_{qq}(z, k_{\perp}; \epsilon) | s' \rangle = \delta_{ss'} C_F \left[\frac{1+z^2}{1-z} - \epsilon(1-z) \right],$$

$$\langle s | \hat{P}_{gq}(z, k_{\perp}; \epsilon) | s' \rangle = \delta_{ss'} C_F \left[\frac{1+(1-z)^2}{z} - \epsilon z \right],$$

$$\langle \mu | \hat{P}_{gq}(z, k_{\perp}; \epsilon) | \nu \rangle = T_R \left[-g^{\mu\nu} + 4z(1-z) \frac{k_{\perp}^{\mu} k_{\perp}^{\nu}}{k_{\perp}^2} \right],$$

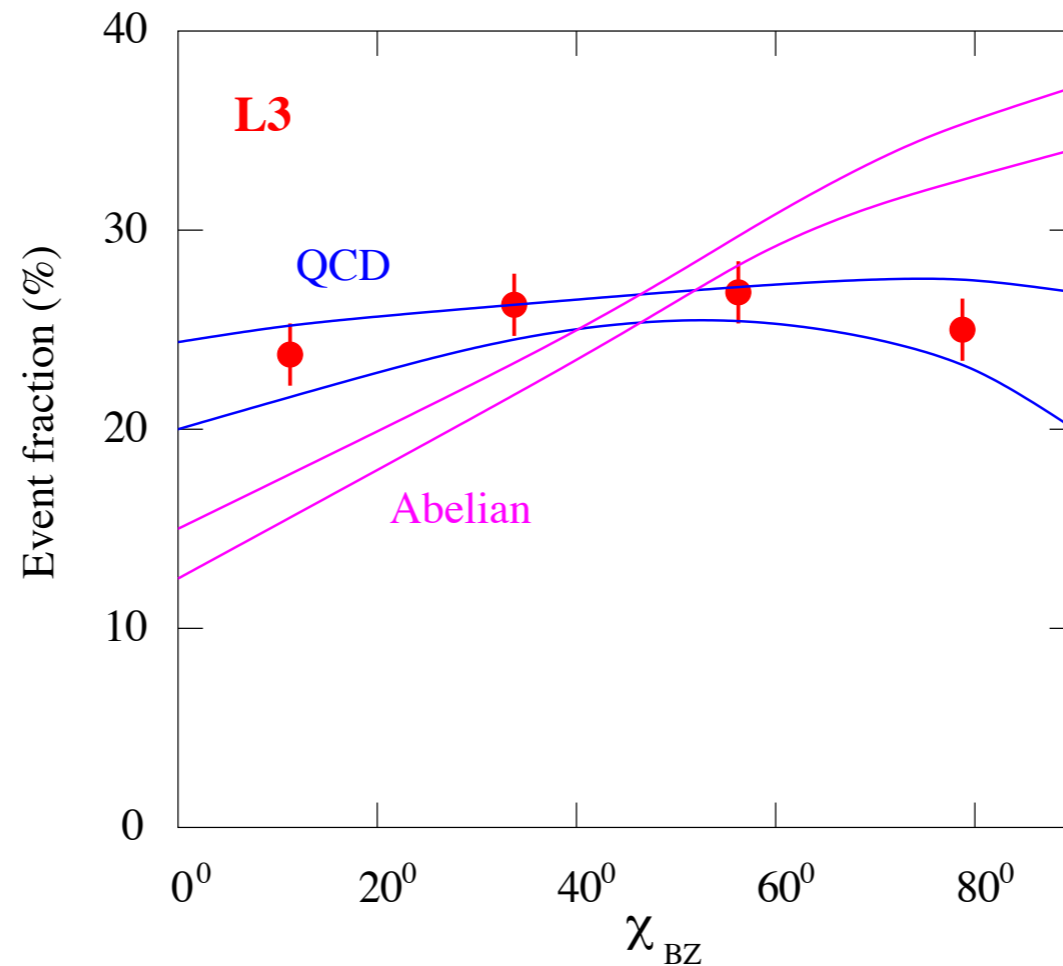
$$\langle \mu | \hat{P}_{gg}(z, k_{\perp}; \epsilon) | \nu \rangle = 2C_A \left[-g^{\mu\nu} \left(\frac{z}{1-z} + \frac{1-z}{z} \right) - 2(1-\epsilon)z(1-z) \frac{k_{\perp}^{\mu} k_{\perp}^{\nu}}{k_{\perp}^2} \right]$$

- No effect in $q \rightarrow qg$ (helicity conservation)
- Opposite in $g \rightarrow gg$ and $g \rightarrow q\bar{q}$
 - ✦ Cancel when $N_f = N_c$

Spin in showers

- Bengtsson-Zerwas angle in $e^+e^- \rightarrow 4$ jets

$$\cos \chi_{BZ} = \frac{(\mathbf{p}_1 \times \mathbf{p}_2) \cdot (\mathbf{p}_3 \times \mathbf{p}_4)}{|\mathbf{p}_1 \times \mathbf{p}_2| |\mathbf{p}_3 \times \mathbf{p}_4|}.$$



- Abelian theory has only $g \rightarrow q\bar{q}$

Conclusions

- Matching at NLO
 - ✦ SM processes automated, EW and BSM soon
- Matching at NNLO
 - ✦ So far only DY & H, others much harder
- Merging at NLO
 - ✦ Still in a state of flux; FxFx automated
- Parton showers
 - ✦ Coherence effects visible
 - ✦ Spin and subleading colour effects small
 - ✦ Hadronization important, but little effort/progress

Thanks for listening!